BELGIAN ROAD RESEARCH CENTRE
Institution recognized by application of the Decree-Law of 30.01.1947
BOULEVARD DE LA WOLUWE 42, B-1200 BRUSSELS

Final report

RESEARCH CONTRACT NO/C3/004

PROPOSAL FOR A EUROPEAN STANDARD IN RELATION WITH THE SKID RESISTANCE OF ROAD SURFACINGS

Coordinator and Reporter: Guy DESCORNET, DSc

May 1998

CENTRE DE RECHERCHES ROUTIERES

ETABLISSEMENT RECONNU PAR APPLICATION DE L'ARRETE LOI DU 30-1-1947
BOULEVARD DE LA WOLUWE, 42 - 1200 BRUXELLES

N/réf.: SSTC/776

CHARLEROI, le 29 juin 1998
Tél.: 071/30.50.05
Fax: 071/30.50.26

SERVICES DU PREMIER MINISTRE
A l'attention de Monsieur J.WAUTREQUIN
Affaires Scientifiques,
Techniques et Culturelles
Rue de la Science 8
1000 BRUXELLES

Monsieur le Secrétaire général,

Objet: Contrat de recherche n° NO/C3/004

J'ai le plaisir de vous transmettre ci-joint en quatre exemplaires, dont deux en français et deux en anglais, le rapport final de la recherche intitulée "Proposition de norme européenne relative à la résistance au dérapage des revêtements routiers", objet du contrat en référence. Le rapport consiste en trois parties séparées, à savoir:

- Le corps du rapport;
- L'annexe 1 sous forme de CD-ROM comportant la base de données constituée au cours de cette recherche (notamment les résultats détaillés), les versions française et anglaise du rapport et un programme de "navigation";
- L'annexe 2 consistant en un projet de norme établi sur base des résultats de la recherche et d'ores et déjà en cours d'examen au sein du groupe de travail européen concerné (CEN/TC227/WG5).

J'ajoute deux copies d'une communication au Symposium tchèque sur les caractéristiques de surface des chaussées (2 juin 1998) dans laquelle les résultats de la recherche et leur utilisation en matière de normalisation européenne sont présentés.

En vous remerciant vivement pour votre soutien, je vous prie de croire, Monsieur le Secrétaire général, à l'assurance de ma haute considération.

G.DESCORNET, Dr.Sc.
Coordinateur

Annexes:
- Rapport en 2 ex. en français + 2 ex. en anglais
- Annexe 1 (CD-ROM) en 4 ex.
- Annexe 2 (Projet de norme) en 4 ex.
- Communication à un symposium en 2 ex.

GHD/ghd

Laboratoires
Fokkersdreef 21 - 1933 Sterrebeek
Boulevard A. Defontaine 10 - 6000 Charleroi

I. Steering Committee membership

Mr R. JORDENS, Eng., Afdelingshoofd, Rijkswaterstaat, Dienst Weg- en Waterbouwkunde (NL), Chairman of CEN/TC227/WG5/TG1.

Mr F. MONTENY, Prime Minister's Office, Scientific, Technical, and Cultural Affairs.

Mr F. BEUGNIES, C.E., Ingénieur-Directeur a.i., Ministère des Communications et de l'Infrastructure, Administration de la Réglementation de la Circulation et de l'Infrastructure (ARCI), Direction Routes: Normes et Banques de Données.

Mr J. WUSTEMBERGHS, Eng., Conseiller, Institut belge de Normalisation.

Mr L. HELEVEN, C.E., Ministerie van de Vlaamse Gemeenschap, Departement Leefmilieu en Infrastructuur (LIN), Administratie Weg en Verkeer, Afdeling Wegenbouwkunde, Dienst Structuren.

Mr J. CROCHET, C.E., Ingénieur principal des Ponts et Chaussées, Ministère wallon de l'Equipement et des Transports (MET), Direction générale des Routes et Autoroutes, Direction des Structures routières.

Mr D. GORLE, Dr, C.E., Directeur, Opzoekingscentrum voor de Wegenbouw (OCW), Departement Research, Ontwikkeling en Toepassing.

Mr G. DESCORNET, DSc, Chef de Projet, Centre de Recherches routières (CRR), Département Recherche, Développement et Application.

II. Acknowledgements

We should like to thank the Prime Minister's Office for Scientific, Technical and Cultural Affairs for funding the project and, in particular, Mr F. MONTENY for his constant attentive support.

We are grateful to LIN and MET for their excellent cooperation to this project, in particular to Mr L. HELEVEN (LIN), J. CHAVET (MET) and J. CROCHET (MET) for carrying out the skid resistance measurements.

Our best thanks are also tendered to the other members of the Steering Committee and especially to Mr R.A.P. JORDENS, who voluntarily made long early morning journeys to attend various meetings including those of the S.C., and to Mr D. GORLE for his sustained occupation with, and effective and friendly chairing of, the S.C.

We gratefully acknowledge the dedication and competence shown by Messrs. J.M. DESMET and B. BERLEMONT in carrying out their technical tasks and handling the large body of data. We owe a particular debt of gratitude to B. BERLEMONT for the making of the appended CD-ROM.

Finally, we thank PIARC for their permission to reproduce excerpts of the data base of the 1st international experiment in Appendix 1 (CD-ROM) for the sake of comprehensiveness.

III. Abstract

There are in Europe over a dozen different models of devices to measure the skid resistance of road surfacings. Up to now each country has been using one or two types of device, with requirements to match in their standard tender specifications and their maintenance policies. The opening up of the single market, however, has created a need for harmonization, to enable any contractor to work to different specifications and road network managers to guarantee homogeneous conditions of safety from one country to the next. This harmonization has been undertaken in CEN - more particularly in group CEN/TC227/WG5. One of the present objectives of this group is to develop a draft standard defining a uniform procedure to determine skid resistance from a dynamic measurement. It will be easily understood that, to be acceptable to a majority of countries, such a procedure can hardly rely on a single device. That is why a philosophy has been adopted to establish equations for converting results produced by different devices, so as to enable anyone to continue to use his or her own method - at least during a period of transition. Anticipating this need, PIARC conducted an international experiment to compare different devices and methods in use to measure friction and surface texture on road and airfield pavements. A final report on this experiment was released by PIARC late in 1995. All devices and methods used in Europe were represented plus one American, two Canadian and two Japanese devices. This experiment produced ample information to set up a large data base, which proves to be a valuable tool in standardization. And the analysis of that information as presented in the final report shows that virtually all devices participating in the experiment can be harmonized using a single equation to relate their outputs to a common scale called (a little prematurely) "International Friction Index" or "IFI", provided allowance is made for a measurement of macrotexture. "Prematurely", because, although this experiment was an indispensable prerequisite, it cannot be used without additional work as a basis to draft a standard that will be acceptable at the European level.

That is why the general objective of this project was to draft a European standard after carrying out the necessary additional work.

As a reminder, the PIARC definition of IFI is as follows:

$$IFI=A+B*F*\exp[(\tau*V-S_R)/(a+b*T)]+C*T$$

where:
- F: the measured friction coefficient
- V: measuring speed
- S_R: reference tyre-road slip speed (60 kmph)
- T: texture depth
- τ: rate of slip
- a, b: empirically determined coefficients to compensate for the influence of speed on the coefficient of friction on the basis of a texture measurement (T)
- A, B, C: empirically determined coefficients specific to each device.

The first task was to resume the analysis of the data base from the PIARC experiment in order to determine the optimum values to be attributed to the parameters used in the definition of IFI. The term "optimum values" was understood to mean those allowing the subset of European devices to reproduce IFI with the greatest possible accuracy. In order that the redefinition of IFI may privilege the measuring equipment and methods actually used in Europe, and with a view to drafting a CEN standard relating to dynamic measurements, twenty-one devices in total were selected according to these two criteria. After the PIARC experiment had been completed, and using data collected in it, an ISO standard 13473-1 was developed defining the way to calculate mean profile depth from profilometer measurements. This work should be taken into account here, all the more as CEN/TC227/WG5 is considering whether to adopt this standard. Now CRR is the only one among the participating teams to have recorded and archived all measured profiles in digital form, which makes it possible to reprocess them by the new technique. Furthermore, it has been necessary to complement the analysis by an evaluation of the repeatability and reproducibility of IFI.

This additional analysis has led us to define a "European Friction Index" or "EFI", which has the following advantages over the IFI proposed by PIARC:

- the role of the texture measurement and, consequently, of the additional errors it may introduce is minimized in two ways. Firstly, a rational choice of the reference speed minimizes the magnitude of the correction to be made for the influence of speed; the optimum reference speed is 30 kmph. Secondly, it has been demonstrated that there is no need to include a texture-dependent term (coefficient C in the equation above) in the definition of EFI for devices fitted with patterned tyres;

- the latter aspect introduces a simplification and, therefore, a fuller harmonization, since, unlike for IFI, the definition of EFI is the same whatever the type of tyre used on a given device;

- EFI takes account of the ISO standard definition of texture depth estimated from a profilometer measurement;

- its definition is based on data relating to (dynamic) European equipment. This data base being more restricted than that of the PIARC experiment, it is possible to obtain values for repeatability and reproducibility which are more representative of the performance levels to be expected from the measuring systems employed in Europe (a knowledge of these values is necessary for the standardization work). The repeatability of EFI has been evaluated at 0.08 on an average for all devices and test sites and its reproducibility between devices at 0.14;

- its main advantage, however, lies in considerably reducing or even eliminating, on the average, the systematic differences in the friction coefficients delivered by the various types of device. This is exactly where the object of harmonization is attained, even at the expense of a lower reproducibility than between devices of the same type.

The second objective of the project was to validate the extension of EFI to other types of surfacing not adequately or not at all considered in the PIARC experiment, by including the various road paving materials and technologies representative of European practice and developments in this field. For that purpose, and with the cooperation of the regional road authorities, skid resistance measurements with the SCRIM of LIN and the odoliograph of MET and texture measurements with the laser profilometer of CRR were performed on twenty-three road sections, 1/3 of which had a conventional surfacing (included as a reference) and 2/3 a surfacing type either recently introduced or more limited in application (such as porous asphalt, porous cement concrete, stone mastic asphalt, chipped resinous slurry, and various other types of thin surfacing). The criterion to be met in validating EFI for a given surfacing was that the latter should obey an empirically established equation which enables the susceptibility of the friction coefficient to the slip speed to be predicted as a function of texture depth. Given the precision of this equation, it can be stated that according to both the PIARC data (except for special cases such as the pavements of two American airfields in Spain) and the data from the additional tests in Belgium, no surfacing type significantly and systematically deviates in one way or another from that relation.

Finally, in pursuance of the third and last objective a draft standard was prepared which:

1) defines EFI, i.e. the equation to change over from one measuring method to another while stating the margin of error associated with this conversion. The equation is essentially the same as above, but the corresponding coefficients have been recalculated and coefficient C has been omitted;

2) proposes a procedure for calibrating friction devices based on EFI. To maintain EFI, it is enough to periodically convene small subsets of (two or three) devices for mutual comparison and adjustment of their coefficients A and B. But these meetings of devices should be organized in such a way as to prevent any subsets from gradually drifting from one another, by observing certain criteria for the pairing of devices.

A first draft of this standard was presented to CEN/TC227/WG5 during the November 21-22, 1997 meeting of this group in Brussels. An amended version including the comments of the group was presented at the meeting of May 25-26, 1998 and it is the third draft prepared after this meeting which is appended to this report as a separate document.

To fully benefit from the work achieved, the following may be recommended.

1. The demonstration of the feasibility of converting the various skid resistance measurements practiced in Europe to a common scale should be disseminated and used as a decisive argument for standardization bodies, road managers, road contractors, suppliers of road construction materials and suppliers of measuring equipment to adopt a policy of "harmonization" rather than "standardization". Harmonization by applying the EFI concept will enable users to continue to use their own tests and to feed their road data bases without breaking with the past and giving up large investments and long-standing experience in the process, as would be the case with the standardization of a single method. This need not keep anyone from preparing the development of a single test method at the European level or in a more general international context over the next fifteen or twenty years. The use of EFI will then have permitted a transition process which may be qualified as "democratic".

2. This requires that the scientific, administrative and political authorities concerned should support the urgent setting up of a European organization for the regular calibration of skid resistance devices as suggested in the draft standard. This organization would not need to have reference test tracks at its disposal; the draft standard makes no requirement to that effect, as comparisons between devices can, in principle and in general, take place in any country or region of Europe as long as the criteria set in the standard are satisfied. The main thing is to have a full-time team dedicated to the organization of tests, the interpretation of results, the issuing of certificates, etc., and capable of moving to the site which is considered to be most appropriate from a practical and economic point of view for convening a given subset of (probably most often two or three) devices.

IV. Abbreviations

B	Blank (or "smooth") tyres
BB	Asphalt (asphalt concrete)
BC	Concrete (cement concrete)
BD	Porous concrete
BFC	Braking force coefficient
CEN	European Committee for Standardization
CRR	Centre de recherches routières (= OCW)
E	Surface dressing
ED	Porous asphalt
EFI	European Friction Index
ESHP	High-performance surface dressing
ETD	Estimated texture depth determined from MPD
IFI	International Friction Index
ISO	International Standardization Organization
LIN	Dienst Leefmilieu en Infrastructuur
MET	Ministère wallon de l'Equipement et des Transports
MPD	Mean profile depth
MTD	Mean texture depth by volumetric method
G	Designates the full set of devices without distinction by tyre type
	OCW Opzoekingscentrum voor de Wegenbouw (= CRR)
PIARC	World Road Association
RMD	Gap-graded thin surfacing
RMS	Root-mean-square of texture profile
RMTO	Open-textured thin surfacing
RP	Ribbed or otherwise patterned tyres
RUMG	Coarse-graded ultrathin surfacing
SCRIM	Sideways Force Coefficient Routine Investigation Machine
SCRIMTEX	SCRIM with added texture-measuring laser profilometer
SFC	Sideways force coefficient
SMA	Stone mastic asphalt
SSTC	Office for Scientific, Technical and Cultural Affairs

V. Symbols

μ	Mean
ρ	Correlation coefficient
σ	Standard deviation
τ	Rate of slip
A, a	Intercept of a regression line
B, b	Slope of a regression line
E	Estimated EFI value
F	Friction coefficient
$F_{10},\ldots,F_{90}$	Value of friction coefficient reduced to a slip speed of 10, ..., 90 kmph
F_S	Value of friction coefficient reduced to slip speed S
F_o	Friction coefficient extrapolated to zero speed
i	Index varying with the device considered
j	Index varying with the half section considered
J	Total number of half sections
m	Index representing the sequence number in a series of measurements performed with a given device on a given half section
n	Number of measurements considered in calculating a regression
N	Total number of devices
R	Index characterizing a value which depends on the choice of S
r	Repeatability
R	Reproducibility R
S	Slip speed
S_o	Parameter describing the influence of slip speed on the friction coefficient; more simply referred to as "speed parameter"
S_o^*	Optimum speed parameter for a given half section
S_o^{**}	Optimum speed parameter predicted from texture
S_R	Reference slip speed
T	Texture depth
x	Index varying with the type of texture measurement considered

VI. Introduction

There are in Europe over a dozen different models of devices to measure the skid resistance of road surfacings. Up to now each country has been using one or two types of device, with requirements to match in their standard tender specifications and their maintenance policies. The opening up of the single market, however, has created a need for harmonization, to enable any contractor to work to different specifications and road network managers to guarantee homogeneous conditions of safety from one country to the next. This harmonization has been undertaken in CEN - more particularly in group CEN/TC227/WG5, of which R. JORDENS, J. CHAVET, L. HELEVEN and G. DESCORNET are members. One of the present objectives of this group is to develop a draft standard defining a uniform procedure to determine skid resistance from a dynamic measurement. It will be easily understood that, to be acceptable to a majority of countries, such a procedure can hardly rely on a single device. That is why a philosophy has been adopted to establish equations for converting results produced by different devices, so as to enable anyone to continue to use his or her own method - at least during a period of transition. Anticipating this need, PIARC conducted an international experiment to compare different devices and methods in use to measure friction and surface texture on road and airfield pavements. A final report on this experiment was released by PIARC late in 1995. All devices and methods used in Europe were represented plus one American, two Canadian and two Japanese devices. This experiment produced ample information to set up a large data base, which proves to be a valuable tool in standardization. And the analysis of those data as presented in the final report shows that virtually all devices participating in the experiment can be harmonized using a single equation to relate their outputs to a common scale called (a little prematurely) "International Friction Index" or "IFI", provided allowance is made for a measurement of macrotexture. "Prematurely", because, although this experiment was an indispensable prerequisite, it cannot be used without additional work as a basis to draft a standard that will be acceptable at the European level.

The general objective of this project was to draft a European standard after carrying out the necessary additional work, which consisted in:

1) resuming the analysis of the data base while restricting it to the dynamic devices used in Europe and reconsidering the reference speed empirically adopted in the definition of IFI with a view to redefining an IFI optimized for European standardization, i.e. an EFI;

2) complementing the analysis by an evaluation of the repeatability and reproducibility of EFI;

3) extending the validity of EFI to new types of surfacing and material not adequately or not at all considered in the PIARC experiment. This required a programme of friction and texture measurements with the various devices available in Belgium on a selected representative sample of different types of

surfacing.

The draft standard was to:

1) define EFI, i.e. the equation to change over from one measuring method to another while stating the margin of error associated with this conversion;
2) propose a procedure for calibrating friction devices.

VII. Analysis of the data base from the international experiment (PIARC, 1992)

As explained above, the purpose of this analysis was to determine, from data collected in the PIARC experiment, the optimum values to be attributed to the parameters used in the definition of the "International Friction Index" or "IFI" proposed in the report on that experiment. The term "optimum values" was understood to mean those allowing the subset of European devices to reproduce IFI with the greatest possible accuracy.

VII.1 Selection of the series of measurements to be considered

In order that the definition of EFI may privilege the measuring equipment and methods actually used in Europe, the following files[1] were selected - in agreement with the Steering Committee[2] - from the PIARC experiment data base. Furthermore, with a view to drafting a CEN standard relating to dynamic measurements, static test methods were excluded from the analysis.

VII.1.1 Friction

Selected files:

B1LKD.FR	B2SLP.FR	B5SLP.FR	C5.FR	C9.FR	D2.FR	D5.FR
B1SLP.FR	B3.FR	C1.FR	C6E.FR	C10.FR	D3.FR	D6.FR
B2LKD.FR	B5LKD.FR	C3B.FR	C8.FR	D1E.FR	D4.FR	D8.FR

Discarded files:

A12.FR Not European. Moreover did not operate correctly.
A13.FR Not European.
A14.FR Pendulum. Not dynamic nor full-scale.
B1ABS.FR ABS system. Actual slip speed unknown.
B4ESLP.FR Though European, not selected because the conditions of measurement are not "pure" (mixture of fixed slip speed and variable rate of slip).
B4ESWP.FR Though European, not selected because the conditions of measurement are not pure (mixture of fixed slip speed and variable rate of slip, making the PIARC model inapplicable).
B5ABS.FR ABS system. Actual slip speed unknown.
B6501.FR Not European.
B6524.FR Not European.

---

[1] *To save space, the various test methods are referred to by the identification codes used in the report on the international experiment. The names of the corresponding devices, with the nationalities of the measuring teams and the types and characteristics of measurement, are presented in* ***Table 1*** *and* ***Table 2*** *for skid resistance and texture, respectively.*

[2] *Minutes of the meeting of the Steering Committee held on November 14, 1996.*

B6CHP.FR Not European.
B6ULT.FR Not European.
B7.FR Pendulum. Not dynamic nor full-scale.
B10E.FR Performed measurements on only four sites.
C3E.FR Many erroneous measurements due to a mechanical problem (see the poor correlation coefficients with other SCRIM devices in the PIARC report [**ref. 1, p. 105**]).
C4.FR Not European.
D7B.FR Performed measurements on only thirteen sites and the results were generally poorly correlated with the outputs of the other devices.

A total of twenty-one devices was thus selected.

VII.1.2 Texture

Selected files[3]:

A1.TX	A3E.TX	D2.TX	D5.TX
A2.TX	A4.TX	D3.TX	
A3B.TX	A5.TX	D4.TX	

Discarded files:

A8.TX Static test. Non-European standard.
A12.TX Not European. Moreover did not operate correctly.
B8.TX Static test.
B11E.TX Static test. Non-European standard.

After the PIARC experiment had been completed, and using data collected in it, an ISO standard 13473-1 [**ref. 2**] was developed defining the way to calculate mean profile depth from profilometer measurements. This work should be taken into account here, all the more as CEN/TC227/WG5 is considering whether to adopt this standard. Now CRR is the only one among the participating teams to have recorded and archived all measured profiles in digital form, which makes it possible to reprocess them by the new technique. Though not really dynamic, the stationary version of CRR's laser profilometer (A5) was selected as it is actually mobile (towed at low speed by a vehicle) and mainly because it is more precise than the truly dynamic version (A4).

VII.1.3 Sites

As explained in the PIARC report, each test site was composed of two adjacent half sections each 75 m long, with half section B following half section A. Site 3 being discarded as it was tested by only one device, we had a total of 106 half sections.

---

[3] *A3B.TX was selected in spite of its non-European (Canadian) origin, as several units of this device are in use in Europe.*

VII.2 Data processing

The PIARC experiment data base comprises a series of (ASCII) files having the extension .FR or .TX for the results of friction or texture measurements, respectively[4]. The data selected was processed in the following stages.

1. Each *.FR file was complemented by a column entitled "RELSP" (for "relative speed"), giving for each individual measurement the actual slip speed, S, as determined by the appropriate equation:

$S = V \sin(\alpha)$ for SFC-type devices, where Ó = yaw angle;
$S = \tau V$ for BFC-type devices, where τ = rate of slip (for locked wheel measurements, $\tau = 1$).

2. For each half section (A and B) and for each device, the linear regression

$$\ln(F_{mij}) = A_{ij} + B_{ij} * S_{mij}$$

where F is the measured friction coefficient and S the relative slip speed, was calculated by means of the least squares method. The following results were archived:

A_{ij}: intercept,
B_{ij}: slope,
ρ_{ij}: correlation coefficient,
σ_{ij}: residual standard deviation,
n_{ij}: number of points,
m: sequence number of the measurement in the series,
i: apparatus considered,
j: half section considered.

These regressions were not used in the subsequent calculations to determine EFI. They were used to verify for each case the validity of the exponential "PIARC" model. After a visual examination of the graph of each exponential equation

$$F = F_0 * \exp(- S/S_0)$$

where $F_0 = \exp(A_{ij})$ and $S_0 = - 1/B_{ij}$, the series of measurements exhibiting an anomaly such as an erratic point, a zero or positive slope, a number of data smaller than three or concentrated in too narrow a range of speeds, etc. were discarded. Only nineteen such outlying series were found (in a total of over two thousand series) :

---

[4] *These initial data being the property of PIARC, it has not been reproduced in Appendix 1 (on the CD-ROM), which essentially contains the results from our new analyses.*

Device	Half section
B1SSLP:	26.2A
B3:	24.A, 24B
C10:	63B
D2:	62A
D4:	26.A, 26.2B, 68A, 81.2B, 81.31, 81.4B
D5:	26.2A, 26.2B, 33.3A, 33.3B, 81.1A, 81.2A
D6:	17B
D8:	19B

A normal series and an outlying series are shown in **Figure 1** and **Figure 2**, respectively. All graphs are visible in **Appendix 1** (on the CD-ROM).

3. A result file *.FR' listing the half sections with the corresponding parameters A, B, F, F_0, S_0, ρ, σ and n was associated with each *.FR file. All these results, including those which were discarded, have been tabulated in **Appendix 1**.

4. The *.FR' files were complemented with columns F_{10}, F_{20}, F_{30}, F_{40}, F_{50}, F_{60}, F_{70}, F_{80} and F_{90}, i.e. the F values recalculated for the S values from 10 to 90 kmph, to put the results in order and to archive them with a view to subsequent visualization and printing - if necessary - of the graphs corresponding with the series of measurements and representing their parameters and regression curves. These results have been tabulated in **Appendix 1**.

5. All the texture data measured with the CRR laser profilometer (device A5) were reprocessed into new values for MPD (mean profile depth) according to ISO standard 13473-1. The symbol used for this new variable is T_{A5ISO}. The old T_{A5MPD} and new T_{A5ISO} values averaged per half section are presented in **Table 3** and have been plotted against each other in **Figure 3**. The regression between the two can be written as :

$$T_{A5ISO} = 0.04 + 0.78 * T_{A5MPD}$$

with a correlation coefficient of 0.988 and a virtually negligible residual standard deviation and ordinate at the origin. A proportionality relation

$$T_{A5ISO} / T_{A5MPD} = 0.78$$

can, therefore, be adopted.

6. A "TEXTURE" file was created giving for each half section the various measurements of texture[5] [6] produced by the selected devices (see above) plus A5/ISO :

---

[5] *For A3B, we have the average values for the three operating speeds: 30, 60 and 80 kmph.*

[6] *For A42, each half section was attributed the average value over the pair of two half sections, as this was the only value provided by the device.*

A1/RMS	A2/RMS	***A2/MPD***	A2/TDMA	A3B/TX1	A3B/TX2
A3E/RGH1	A42/RMS	A42/MPD	***A5/MPD***	D2/MTD	D3/RA
D3/RQD4/CSMTD	D5/SMTD	***A5/ISO***			

The three files in bold italic have been reproduced in **Appendix 1**.

7. Eleven files called "TabX" were created giving for each site/section the "X" value produced by each device (one column per device), with $X = S_o, F_o, F_{10}, \ldots, F_{90}$. F_S values for which the slip speed, S, was outside the actual measuring range of the apparatus were discarded, except those corresponding with the decade just below and the decade just above that range. These files have been reproduced in **Appendix 1**.

8. From the initial data files (one file per device, comprising 52 pages each reporting the data measured on two half sections):

- the average of the ln(F) values, $\langle \ln F \rangle_{ij}$, and the average of the S values, $\langle S \rangle_{ij}$, were calculated and the number n_{ij} of measurements was selected for each series of measurements (m) per device (i) and per half section (j);

- from this point onwards, the calculations were made separately for the subset of devices using smooth tyres, the subset of those with patterned tyres and the two combined, leading to a systematically triple presentation of results with the notations G for overall, B for blank (or smooth), and RP for ribbed or otherwise patterned;

- for some fifty S_o values ranging from 10 to 500 by geometric progression, the residual standard deviations, σ_{ij}, of the series of measurements $\{ F_{mij} \}$ from the equation curve

$$F = EXP\{\langle \ln F \rangle_{ij} - (S - \langle S \rangle_{ij})/S_o\}$$

were calculated. In a graph showing lnF versus S, this curve becomes a line with a variable slope passing through the centre of gravity of the points representing the data measured by the device considered on the half section considered. These graphs are visible in **Appendix 1**;

- for each half section (j), the overall average residual standard deviation

$$\langle \sigma \rangle_j = SQRT\{ \sum_i n_{ij}\sigma_{ij}^2 / \sum_i n_{ij} \}$$

was calculated for each S_o value;

- for each half section (j), $\langle \sigma \rangle_j$ was plotted against S_o and the S_o value minimizing $\langle \sigma \rangle_j$, S_{oj}^*, was determined (by parabolic interpolation between the lowest three points) - see the example of **Figure 4**. These graphs are visible in **Appendix 1**.

In this way of determining an "average" S_o value characteristic of a half section but common to all devices, each individual measurement is accounted for with the same weight. More particularly, the influence of the deviation of a given measurement from the model is the same for all measurements whichever device is considered, whatever the measuring speed and whatever the number of measurements performed by the device on the site. This method differs from that described in the report on the PIARC experiment [**ref. 1, p. 128**], which simply averages the S_o values found by regressive fitting of the exponential model to each series of measurements made by a given device on the site considered; in our processing scheme, this would amount to taking the average of the S_{oij} values of each device as the optimum value S_{oj}^*, using the equation:

$$S_{oj}^* = \Sigma_i (-1/B_{ij}) / \Sigma_i n_{ij}$$

Now this method introduces two sorts of biases.

Firstly, high S_o values are given more weight than low values. At worst, it would take only one friction coefficient virtually not decreasing with speed to have a corresponding S_o value tending to infinity, thereby determining the average value all by itself.

Secondly, the S_o values found for devices operated at low slip speed are more sensitive to errors in measurements of F than those calculated over a wider range of speeds, whereas they are given the same weight.

The method adopted here gives exactly the same weight to each individual measurement and the optimum S_o value for a given half section is that minimizing the sum of the squares of all deviations from the F(S) curves.

Figure 5 presents an example of the fitting of exponential curves of equal slope to a set of series of data measured with different devices on a given half section.

9. For all reference speeds S_R ranging from 10 to 90 kmph with intervals of 10 kmph, the following operations were performed :

- for each measurement (measurement m, device i, half section j): separate calculation and tabulation, with the corresponding slip speed S_{mij} given in the first column, of the value of friction coefficient F_{Rmij} reduced to the reference speed, using the equation:

$$F_{Rmij} = \exp\{\ln F_{mij} - (S_R - S_{mij})/S_{oj}^*\}$$

- averaging the F_{Rmij} values over all devices for each half section:

$$\langle F_R \rangle_j = \Sigma_m \Sigma_i F_{Rmij} / \Sigma_i n_{ij}$$

This value corresponds with the "golden" (ideal) value defined in the report on the PIARC experiment [**ref. 1, p. 127**]. For each device and each S_R value, F_{Rmij} was plotted against $<F_R>_j$ while representing all half sections on the same graph (**Figure 6**), and parameters A_{Ri}, B_{Ri}, ρ_{Ri} and σ_{Ri} of the linear regression :

$$<F_R>_j = A_{Ri} + B_{Ri} * F_{Rmij}$$

were calculated.

A search was then made for all deviations greater than $3\sigma_{Ri}$ from the regression line; such a deviation being indicative of a systematic wide shift of the series of measurements to which it belonged. The following outlying series were found (see the example in **Figure 7**):

- Graphs without distinction by type of tyre:

C1: 61A, 61B, 82.3A, 82.3B
C5: 66A, 66B
C8: 26.1A, 26.1B, 82.3A
C9: 26.1A, 26.1B
C10: 26.1A, 26.1B, 50A, 50B
D6: 26.1A, 26.1B, 33.1A, 33.1B, 34A, 34B
D8: 81.3A, 81.3B

- Specific graphs for smooth tyres:

C8: 26.1B
D2: 12A, 12B
D6: 26.1A, 34A, 34B, 50B, 53A
D8: 81.3A, 81.3B

- Specific graphs for patterned tyres:

B5LKD: 82.2A, 82.2B, 82.3A, 82.3B
C1: 82.1A, 82.3B.

At this stage of the analysis, these series of data were maintained; we shall see later on whether their removal significantly improved the precision of EFI. All these graphs, including those discarded after the calculations, are visible in **Appendix 1**.

11. The relative and absolute values of the overall residual standard deviation, σ_R, of all measurements were plotted against S_R (**Figure 8**). The relative values prove to slightly increase with S_R, this can be explained by considering that in the diagram of lnF versus S, the prediction of $\langle F_R \rangle_j$ from an F_{Rmij} measurement is made by means of parallel lines having a slope $-1/S_{oj}^*$ and that, consequently, the deviations do not vary with the choice of S_R. Now the relative deviations are nothing else but the deviations on lnF, and that is why the relative σ_R is approximately constant. As for the absolute σ_R, it decreases when S_R increases; likewise, at equal S_o value, the variation between two decreasing exponential curves in the diagram of F versus S decreases when S increases.

12. The graphs representing S_{oj}^* versus texture measurement T_{ISO} were drawn either separately for the devices with smooth tyres (**Figure 9**) and those with patterned tyres (**Figure 10**) or for all devices regardless of tyre type (**Figure 11**). It can be seen that considerably outlying results were found for three sites:

- the two half sections of site 34,
- the eight half sections of site 81,
- the two half sections of site 82.2.

Site 81 is, in fact, the main runway of the NASA air base at Moron (Spain). One explanation could be the observation made by participants that this pavement, which has a relatively fine macrotexture (0.44 mm < T_{ISO} < 0.57 mm), seems to include aggregate obtained from volcanic rock extremely rough to the touch. There are obviously no errors in measurement or abnormal measuring conditions involved, as the S_{oj}^* values were determined from the outputs of all the devices. Special cases like this should be remembered as calling for further investigation. Nevertheless, we have to exclude them from the analysis for the time being. This being done, parameters a_{ISO}, b_{ISO} and σ_{ISO} of the regression[7]

$$S_{oj}^* = a_{ISO} + b_{ISO} * T_{ISO}$$

were calculated, taking the data of device A5 as a basis.

Site 82 is on another NASA base at Rota in Spain. Here the explanation could be local traces of rubber left by the tyres of aeroplanes landing on the test sections. Perhaps those traces were larger or more marked on section 82.2 than on the other two adjacent sections.
Site 34 is the only surfacing of the ESHP type and is made of highly abrasive fine chippings spread on a tack coat in epoxy resin. The case is similar to that of the runway of Moron, though much milder. Moreover, the outliers are limited to smooth-tyred devices.

---

[7] *Index ISO refers to the fact that the data base contains other texture measurements.*

These twelve special half sections were excluded from the analysis. **Figure 12**, **Figure 13** and **Figure 14** show the new graphs "trimmed" of outliers and the results of the updated regressions are presented in **Table 4**. It should be noted that from this point onwards texture depth by the ISO standard will have to be considered.

A remarkable finding here is that none of the three sites in porous asphalt stands out from the rest, as could be expected on account of their peculiar macrotexture. In the PIARC report they were discarded a priori without further justification.

13. Finally, stages 9 and 10 were repeated using S_{qj}^{**} values, i.e. S_{qj}^{*} values predicted from texture depth values determined by the ISO method. This resulted in end values for A_{Ri}, B_{Ri}, ρ_{Ri} and σ_{Ri}.

VII.3 Separation by tyre type

Devices measuring skid resistance by means of a smooth tyre should, in principle, be more sensitive to the macrotexture of the road surfacing under test than those using a patterned tyre, as the former call upon the macrotexture to do all the drainage whereas the latter perform this drainage partly by themselves, through the grooves in their treads. As a result, the parameters of the PIARC model, especially parameter S_0, may be expected to differ significantly on a given site according to the tyre type used. That is why stages 8 to 13 were repeated while distinguishing between devices using a smooth tyre (C3B, C5, C64, C8, C9, C10, D1E, D2, D3, D4, D5, D6, D8) or a patterned tyre (B1LKD, B1SLP, B2LKD, B2SLP, B3, B5LKD, B5SLP, C1). The relations between S_0 and T_{ISO} (**Figure 12** and **Figure 13**) actually appear to differ significantly (from a statistical point of view[8]) according to tyre type. However, the correlation is markedly better when considering all the devices together, regardless of tyre type. The residual standard deviations on S_0 are 20 kmph overall and 21 and 29 kmph for the series corresponding with patterned and smooth tyres, respectively. It should be noted that this finding need not be paradoxical: the S_0 values differ between the three series because they each result from a new least squares fit to the set of series of measurements per half section and per device.

[8] *Using the SNEDECOR-FISHER test for comparing slopes.*

VII.4 Choice of the reference speed

At this stage, the harmonized coefficient of friction - which may be called EFI by now - can be predicted from an individual measurement F_{mij} performed at a speed S_{mij} by means of the equation[9]

$$EFI_j = A_{Ri} + B_{Ri} * F_{mij} * \exp\{(S_{mij} - S_R)/(a_{ISO} + b_{ISO} * T_{ISO})\}$$

The various devices have different ranges of operating speeds. With a device capable of measuring at the reference speed S_R it will be possible to do without knowledge of macrotexture, the fractional exponent in the above equation being reduced to zero. In general, more allowance for the texture measurement will have to be made as the measuring speed, S_{mij}, is different from the reference speed. This means that the greater the difference between the measuring range of a device and S_R, the more any imprecision of a device x used to measure texture will affect (through errors in measuring T_x as well as through the imprecision of the equation to predict S_{oj}^*) the accuracy of EFI prediction with this device. To minimize this source of error, an S_R value must, therefore, be chosen which in a way corresponds to the average of the operating speeds of the various devices. More precisely, this optimum reference speed will be that which minimizes the standard deviation, calculated over all half sections j, of the differences between, on the one hand, EFI_{xj} found with the prediction of S_{oj}^* based on some other texture measurement, T_x, than the standardized ISO measurement - parameters A_{Ri} and B_{Ri} remaining unchanged as they are part of the definition of EFI - and, on the other, its "true" value, $\langle F_R \rangle_j$. The definition of EFI being based on the newly standardized measurement T_{ISO}, the differences in S_{oj}^* predictions between the various selected texture measuring methods and the ISO method can, indeed, be considered as representative of the source of errors due to the texture measurement. The texture measurement files only contain the average values per half section. Neither the differences between measurements replicated at the same location nor the differences between the measurements at locations spread over the section were archived. As a result, the method proposed to determine an optimum value for the reference speed does not take account of the intrinsic errors in measurements (repeatability), but only of the imprecision or uncertainty in the equation to predict S_{oj}^*.

An estimate, E_{Rmixj}, of $\langle F_R \rangle_j$ was thus calculated from all F_{mij} values and for all reference speeds, using the equation

$$E_{Rmixj} = A_{Ri} + B_{Ri} * F_{mij} * \exp\{-(S_R - S_{mij})/S_{oxj}^{**}\}$$

where

$$S_{oxj}^{**} = a_x + b_x * T_{xj}$$

---

[9] *The subscript j affixed to EFI characterizes a half section, whatever the measuring method used.*

giving

$$E_{Rmixj} = A_{Ri} + B_{Ri} * F_{mij} * \exp\{-(S_R - S_{mij})/ (a_x + b_x * T_{xj})\}$$

Then the absolute and relative quadratic means of the differences between E_{Rmixj} and $<F_R>_j$ were calculated by summation over all the friction measurements performed by all the devices on all the sites and further summation over all the texture measurements other than ISO:

$$\sigma_{R,x,abs}=SQRT\{\Sigma_x\Sigma_j\Sigma_i\Sigma_m(E_{Rmixj} - E_{Rmi,ISO,j})^2 / \Sigma_x\Sigma_j\Sigma_i\Sigma_m\ 1\}$$

$$\sigma_{R,x,rel}=SQRT\{\Sigma_x\Sigma_j\Sigma_i\Sigma_m[(E_{Rmixj} - E_{Rmi,ISO,j})/ E_{Rmi,ISO,j}]^2/\Sigma_x\Sigma_j\Sigma_i\Sigma_m\ 1\}$$

The standard deviations found (**Figure 15** and **Figure 16**) as a function of the reference speed exhibit a maximum at roughly S_R = 30 kmph; this value will henceforth be proposed for the definition of EFI. Consequently, it is possible to give the regression parameters enabling each device to predict this EFI, either regardless of tyre type (first part of **Table 5**) or according to it (second part of **Table 5**).

VII.5 Repeatability of EFI

The repeatability of each method to measure F was investigated and reported in the PIARC report [**ref. 1, p. 45**]. The investigation related to variations between measurements replicated under the same conditions, especially of specified speed[10]. What we are interested in here is the repeatability of the EFI value whatever the operating speed, since the allowance made for texture is nothing else but a correction for the influence of speed which reduces EFI to a fixed reference speed. As stated above, we only have replicated measurements for skid resistance and not for texture, for which only average values per half section were archived. This means that the repeatability of EFI considered here is assessed from replicated measurements of F converted in terms of EFI using a single value of T measured on the site considered.

The repeatability of EFI per half section was calculated by means of standardized equations [**ref. 4**]:

$$N = \Sigma_i 1$$
$$n_{ij} = \Sigma_m 1$$
$$\mu_{ij} = \Sigma_m EFI_{est,mij} / n_{ij}$$
$$\sigma_{ij} = SQRT\{\Sigma_m(EFI_{est,mij}-\mu_{ij})^2/(n_{ij}-1)\}$$
$$\sigma_{rj} = SQRT\{\Sigma_i (n_{ij}-1)\ \sigma_{ij}^2 / (\Sigma_i n_{ij}-N)\}$$
$$r_j = 2\sqrt{2}\ \sigma_{rj}$$

[10] *Although the operating speeds were very often rather different from the specified speed, which may have affected the repeatability values found.*

Calculations were made on the one hand on the "trimmed" data (outliers removed) used to define EFI and, on the other, on the "untrimmed" full initial data. The results are presented in **Table 6**. Averaged over all sites, using the standardized equations

$$J = \sum_j 1$$
$$r = \sum_j r_j / J$$

a repeatability of 0.08 to 0.10 is found, according to whether the trimmed or untrimmed data is considered. It should be noted that analysing the devices in one or two separate classes according to tyre type has virtually no influence on the repeatability of EFI.

VII.6 Reproducibility of EFI

Since EFI must be determined from a skid resistance and a texture measurement, its reproducibility depends, strictly speaking, on both types of measurement. In our analysis, it is characterized by the standard deviations of the differences in EFI values - all other relevant things remaining unaltered - between pairs of different measuring systems. "Measuring system" here is understood to mean the association of a method to measure F with a device producing a measurement of T in accordance with the ISO standard. Although both friction and texture measurements may be combined in a single device as in the case of the SCRIMTEX, the devices to measure F and T should not, in principle, be considered as paired but rather as independent, i.e. any method to measure F can be associated, for a given series of measurements, with any method to measure T_{ISO}. This, in any case, is an assumption which puts us on the safe side, by maximizing the possible deviations. Under such conditions, the overall reproducibility of EFI at the optimum reference speed S_R = 30 kmph should be characterized by the variations between pairs of measuring systems (F, T_{ISO}), all possible combinations being included. Unfortunately, our device is the only one capable of producing ISO standard values for the textures considered in the PIARC experiment. Estimating the reproducibility of EFI from varied pairs of measurements (F, T_{ISO}) is, therefore, impossible. As a result, the calculation presented below only takes account of the variations in EFI predictions due to the use of different friction devices, the texture measurement being assumedly performed with a single device. The reproducibility of EFI is then calculated by the following standardized equations [**ref. 4**]:

$$n_j = \{(\sum_i n_{ij})^2 - \sum_i n_{ij}^2\} / \{(N-1) \sum_i n_{ij}\}$$
$$\mu_j = \sum_i n_{ij} \mu_{ij} / \sum_i n_{ij}$$
$$\sigma_{Rj}^2 = \{(\sum_i n_{ij} (\mu_{ij} - \mu_j)^2)/(N-1) - \sigma_{rj}^2\} / n_j$$
$$R_j = 2\sqrt{2}\, \mathrm{SQRT}(\sigma_{Rj}^2 + \sigma_{rj}^2)$$
$$R = \sum_j R_j / J$$

The results are presented in **Table 6**. Depending on whether the results were trimmed of outliers or not, values between 0.14 and 0.17 are found for the overall reproducibility of EFI. Like for repeatability, separate consideration by tyre type does not result in a significant improvement.

The reproducibility of EFI can be assessed from another angle : that of the harmonization between the various measuring methods. Let us take the example of the two Belgian devices which participated in the PIARC experiment - the SCRIM of LIN and the odoliograph of MET - and let us compare the results they produced at the same speed on a given site. **Figure 26** and **Figure 27** show the distributions of differences found between the two measurements, for the friction coefficient (SFC) determined by each device using its own method and for the harmonized friction coefficient (EFI), respectively. It can be seen that the conversion to EFI values not only significantly reduces the average absolute difference (from 0.08 to 0.01) but also leads to a decrease in standard deviation (from 0.08 to 0.05). This virtual elimination of average difference is nothing else but the objective of harmonization, i.e. to enable different devices to express their results on a single common scale of friction coefficient.

VII.7 Accuracy of EFI

There is no such thing as a single absolutely accurate tyre-road friction coefficient, because of the numerous factors involved and the difficulty or even impracticability of defining, maintaining and reproducing reference surfaces and/or tyres which can be used as stable standards. EFI is, in fact, a "floating" standard, which may drift with the set of devices upon which its definition is based. The concept of accuracy of an EFI value is, therefore, meaningless. However, the accuracy of a given device can be considered as the degree of agreement of its output with the EFI value. In this respect, the accuracy of a device i would be nothing else but the residual standard deviation, σ_i, of the regression which determines parameters A_i and B_i as presented in **Table 5**. Averaged over all the devices, the residual standard deviation in predicting EFI is found to be 0.050 (in relative terms : 9.4 %) overall for all tyres and 0.047 (in relative terms : 9.0 %) if the type B and type RP tyres are taken separately.

*VII.8 Sensitivity of EFI to imprecisions in estimating S_{oj} **

The prediction, S_{oj}^{**}, of S_{oj}^{*} from texture depth (**Figure 14**) is affected by an imprecision which can be described by the residual standard deviation from the regression

$$S_{oj}^{**} = a + b * ETD_{ISO}$$

This deviation, σ_{Sp}, has a value of 20 kmph after the outliers have been discarded. The resulting imprecision in predicting EFI will depend on the difference between the operating speed (actual slip speed) and the reference (slip) speed of 30 kmph, as well as on the friction level measured. The standard deviation, σ_{EFI}, of this source of potential errors can be derived from the equation relating EFI to S_p :

$$\sigma_{EFI} = \sigma_{Sp} * B * F * ((30-S)/(S_{oj}^{**})^2) * \exp((S-30)/S_{oj}^{**})$$

or, in general terms, since A and B are close to zero and unity, respectively, and after replacing σ_{Sp} with its value and eliminating F in order to include EFI:

$$\sigma_{EFI} = 20 * EFI * ABS((30-S)/(S_{oj}^{**})^2)$$

The values of σ_{EFI} are presented in **Table 10** through **Table 15**.

VIII. Additional measurements (SSTC, 1997)

As stated before, the objective of these measurements was to try and extend the validity of IFI to road surfacings having an anisotropic texture (grooved cement concrete), to open-textured surfacings (porous asphalt, open-textured thin surfacing, gap-graded thin surfacing, coarse-graded ultrathin surfacing) and to special materials (high-performance surface dressing), which had not been adequately considered in the PIARC experiment. This required a programme of additional road tests.

VIII.1 Selection of sites

The twenty-five sites selected for the measurements are presented in **Table 7**. The sample was composed of eight conventional surfacings (one surface dressing, three type I (dense) asphalts, and four exposed aggregate concretes) and seventeen special surfacings (four porous asphalts, one high-performance surface dressing, one porous (cement) concrete, one type II (dense) asphalt 0/10, one fine-graded exposed aggregate (cement) concrete 0/7, five open-textured thin surfacings, two coarse-graded ultrathin surfacings, one gap-graded thin surfacing, and one grooved (cement) concrete).

VIII.2 Equipment used

The devices used were the odoliograph of MET and the SCRIMTEX of LIN. The former already participated in the PIARC experiment, while the latter was a new device having, in principle, the same characteristics and performance as the SCRIM of LIN which participated in the PIARC experiment.

VIII.3 Implementation

All the planned measurements were actually performed except on sites 15 and 25, which had become impracticable at the time of testing. The skid resistance measurements took place from 1st till 7th April 1997, and the texture measurements from 8th April till 21st May 1997. The conditions of measurement were strictly the same as in the PIARC experiment. More particularly, the sections of 150 m were divided in two and results were reported for each half section of 75 m. The skid resistance measurements were repeated by making two runs at each of the specified three speeds (30, 60 and 90 kmph). The texture measurements were made on four locations in each half section and the average values were reported.

VIII.4 Results

The results are given in **Appendix 1**. The reduced data, i.e. the parameters of the exponential regression between the friction measurements and slip speed, are reviewed in **Table 8** and **Table 9**.

In **Figure 24** and **Figure 25**, comparisons based on the SCRIM and the

odoliograph measurements, respectively, are made between the correlations of the speed parameter, S_{oij}, with texture depth, T_{ISO}, found on the set of PIARC sites and on the set of SSTC sites. It can be seen that, as far as the SCRIM is concerned (**Figure 24**), the two superimposed sets roughly coincide, both in range of values and in scatter. The latter observation tends to show that, although they generally differ in nature from the PIARC sites, the surfacings included in the SSTC selection virtually obey the same relation between S_0 and T. As for the results from the odoliograph measurements (**Figure 25**), the set of SSTC points coincides reasonably well with the PIARC set, except for seven points corresponding with two complete sections (one in porous concrete, the other in SMA) and three half sections (in SMA, exposed aggregate concrete and RUMG). With the exception of the latter two, these seven half sections belong to the test site at Herne and were tested on the same day. Since the correlation obtained with the same devices in the PIARC experiment is actually found again, and since the few exceptions reported above do not appear in the SCRIM measurements, care must be taken in drawing final conclusions for those uncertain cases. On the other hand, it will be noted that, contrary to expectation[11], the porous asphalt surfacings did not exhibit any peculiar behaviour - neither in the PIARC nor in the SSTC experiment. Finally, according to the SCRIM and the odoliograph measurements, respectively, the S_0 value on the high-performance surface dressings is either too high or too low with respect to the T_{ISO} value. In both cases, however, the corresponding points remain within the limits of the scatter found in the PIARC experiment for all surfacings except the ESHP. The case of the ESHPs is, therefore, not clear, since they cannot, in general, be said to deviate in one way or the other from the average behaviour of the other surfacings.

A comparison of the distributions of the differences in values provided by the two devices in terms of SFC (**Figure 28**) and EFI (**Figure 29**) confirms the effectiveness of harmonization, as the conversion to EFI reduces both the average absolute difference and the standard deviation.

[11] *Although the PIARC report does not say anything about them as they were automatically excluded from the analysis.*

IX. Proposal for a standard

As explained earlier, the general objective of the project was to submit a draft defining EFI and specifying a calibration procedure to the CEN group TC227/WG5.

A first draft was presented during the November 21-22, 1997 meeting of this group in Brussels. An amended version including the comments of the group was presented at the meeting of May 25-26, 1998 and it is the third draft prepared after this meeting which is appended to this report as a separate document (**Appendix 2**).

One question raised during the March 1996 meeting of CEN/TC227/WG5 plunged the group into perplexity. The Danish representative wondered why the exponential curve did not reflect the well-known phenomenon of the existence of a maximum friction coefficient in the low speed range - a phenomenon which is utilized for example by ABS systems. This seemed to be a serious objection which threatened to disprove the basic line of argument of the PIARC report. A direct reply could have been made by plotting the regression curves or at least giving the residual deviations found in applying the model to the results of the PIARC experiment. But for a trivial reason, viz. that it would have been necessary to individually examine more than two thousand graphs, this question had not been clearly solved in the PIARC report. Our first task was, therefore, to systematically recalculate all the regressions while displaying each time the corresponding graph in order to visually detect any anomaly. Only nineteen out of the two thousand and odd regressions exhibited either excessive deviations (in fact barely greater than one sigma) or an exponential curve with a positive or virtually zero slope (**Figure 2**). A sign of the existence of a maximum at low speed was nowhere to be found, which confirms the validity of the exponential model (**Figure 1**).
In fact, there seems to be confusion between two test conditions: either variable speed and constant rate of slip - as in the PIARC experiment -, in which case the exponential model applies; or constant speed and variable rate of slip, in which case a maximum is observed not at low speed but at a low rate of slip, and the exponential model no longer applies; another model which was recently proposed [**ref. 3**] can then be used (**Figure 17** to **Figure 22**).

In the meantime we have found a reference dated 1966, in which a diagram is presented (**Figure 23**) which is very similar to the synthesis proposed in **Figure 19**.

X. Conclusions

The analysis performed on the European devices in the PIARC data base has shown that:

- the PIARC model based on a decreasing exponential relation between F and S with a slope independent of the measuring method allows the results to be described with good approximation;

- parameter S_0 in the model can be predicted, with adequate approximation for the intended application, from a texture measurement;

- it has been possible to establish this relation between S_0 and macrotexture on the basis of a new standardized ISO definition of mean texture depth, after reprocessing our records of laser texture measurements saved from the PIARC experiment;

- the reference slip speed S_R can be defined in such a way as to minimize the influence of the correction for speed on EFI. This optimum speed is 30 kmph.

With the above findings it is possible to define an EFI which has the following advantages over the IFI proposed by PIARC:

- the role of the texture measurement and, consequently, of the additional errors it may introduce is minimized in two ways. Firstly, a rational choice of the reference speed minimizes the magnitude of the correction to be made for the influence of speed. Secondly, it has been demonstrated that there is no need to include a texture-dependent term in the definition of EFI for devices fitted with patterned tyres;

- the latter aspect introduces a simplification and, therefore, a fuller harmonization, since, unlike for IFI, the definition of EFI is the same whatever the type of tyre used on a given device;

- EFI takes account of a standardized definition of texture depth estimated from a profilometer measurement which is more recent than IFI concept;

- its definition is based on data relating to (dynamic) European equipment. This data base being more restricted than that of the PIARC experiment, it is possible to obtain values for repeatability and reproducibility which are more representative of the performance levels to be expected from the measuring systems employed in Europe (a knowledge of these values is necessary for the standardization work).

The repeatability of EFI has been evaluated at 0.08 on an average for all devices and test sites and its reproducibility between devices at 0.14.

The main advantage of EFI, however, lies in considerably reducing or even eliminating, on the average, the systematic differences in the friction coefficients delivered by the various types of device. This is exactly where the object of harmonization is attained, even at the expense of a lower reproducibility than between devices of the same type.

As for the objective of extending the validity of EFI to other types of surfacing not considered in the PIARC experiment, it can be said that, in view of the precision of the relation between the speed parameter, S_o, and texture depth, T_{ISO}, and with the exception of two American airfield pavements in Spain, neither the analysis of the PIARC data nor the additional tests made in Belgium have revealed any type of surfacing which significantly and systematically deviates in one way or the other from that relation.

Finally, this study has laid the foundation(s) of a proposal for a European standard defining EFI and specifying its calibration procedure, which was submitted in November 1997 to the CEN group TC227/WG5 and is under discussion in this group.

XI. Recommendations

1. The demonstration of the feasibility of converting the various skid resistance measurements practiced in Europe to a common scale should be disseminated and used as a decisive argument for standardization bodies, road managers, road contractors, suppliers of road construction materials and suppliers of measuring equipment to adopt a policy of "harmonization" rather than "standardization". Harmonization by applying the EFI concept will enable users to continue to use their own tests and to feed their road data bases without breaking with the past and giving up large investments and long-standing experience in the process, as would be the case with the standardization of a single method. This need not keep anyone from preparing the development of a single test method at the European level or in a more general international context over the next fifteen or twenty years. The use of EFI will then have permitted a transition process which may be qualified as "democratic".

2. This requires that the scientific, administrative and political authorities concerned should support the urgent setting up of a European organization for the regular calibration of skid resistance and texture devices as suggested in the draft standard. This organization would not need to have reference test tracks at its disposal; the draft standard makes no requirement to that effect, as comparisons between devices can, in principle and in general, take place in any country or region of Europe as long as the criteria set in the standard are satisfied. The main thing is to have a full-time team dedicated to the organization of tests, the interpretation of results, the issuing of certificates, etc., and capable of moving to the site which is considered to be most appropriate from a practical and economic point of view for convening a given subset of (probably most often two or three) devices.

XII. Tables

TABLE 1 - FRICTION DEVICES PARTICIPATING IN THE PIARC EXPERIMENT. THE EUROPEAN DEVICES SELECTED FOR DEFINING EFI ARE IN GREY TINT BLOCKS 33
TABLE 2 - TEXTURE DEVICES PARTICIPATING IN THE PIARC EXPERIMENT. THE EUROPEAN DEVICES SELECTED FOR DEFINING EFI ARE IN GREY TINT BLOCKS 35
TABLE 3 - COMPARISON BETWEEN THE MPD VALUES DETERMINED IN THE PIARC EXPERIMENT USING THE CRR PROCESSING METHOD AND THE MPD VALUES CALCULATED FROM THE SAME DATA USING THE ISO STANDARD METHOD ISSUED AT A LATER DATE 36
TABLE 4 - PARAMETERS OF THE LINEAR REGRESSION $S_{OJ}^* = A_{ISO} + B_{ISO} * T_{ISO}$ 37
TABLE 5 - PARAMETERS OF THE REGRESSIONS ENABLING EACH DEFICE TO PREDICT EFI. 37
TABLE 6 - REPEATABILITY, R_J, AND REPRODUCIBILITY, R_J, OF EFI PER HALF SITE J 38
TABLE 7 - SITES FOR THE ADDITIONAL MEASUREMENTS IN BELGIUM. 41
TABLE 8 - RESULTS OF THE ADDITIONAL MEASUREMENTS IN BELGIUM WITH THE SCRIM OF LIN 42
TABLE 9 - RESULTS OF THE ADDITIONAL MEASUREMENTS IN BELGIUM WITH THE ODOLIOGRAPH OF CRR 43
TABLE 10 - STANDARD DEVIATION OF THE ERROR IN EFI DUE TO IMPRECISION IN PREDICTING S_P FROM TEXTURE WITH S_P = 50 KMPH, WHICH CORRESPONDS WITH MTD≅0.0 MM (ABSENCE OF MACROTEXTURE). 44
TABLE 11 - STANDARD DEVIATION OF THE ERROR IN EFI DUE TO IMPRECISION IN PREDICTING S_P FROM TEXTURE WITH S_P = 75 KMPH, WHICH CORRESPONDS WITH MTD≅0.3 MM. 44
TABLE 12- STANDARD DEVIATION OF THE ERROR IN EFI DUE TO IMPRECISION IN PREDICTING S_P FROM TEXTURE WITH S_P = 100 KMPH, WHICH CORRESPONDS WITH MTD≅0.75 MM. 45
TABLE 13 - STANDARD DEVIATION OF THE ERROR IN EFI DUE TO IMPRECISION IN PREDICTING S_P FROM TEXTURE WITH S_P = 150 KMPH, WHICH CORRESPONDS WITH MTD≅1.5 MM. 45
TABLE 14 - STANDARD DEVIATION OF THE ERROR IN EFI DUE TO IMPRECISION IN PREDICTING S_P FROM TEXTURE WITH S_P = 200 KMPH, WHICH CORRESPONDS WITH MTD≅2.5 MM. 46
TABLE 15 - STANDARD DEVIATION OF THE ERROR IN EFI DUS TO IMPRECISION IN PREDICTING S_P FROM TEXTURE WITH S_P = 250 KMPH, WHICH CORRESPONDS WITH MTD≅3.5 MM. 46

Table 1 - Friction devices participating in the PIARC experiment. The European devices selected for defining EFI are in grey tint blocks

DEVICE		MEASUREMENT TYPE	TYRE TYPE (1)	RATE OF SLIP (%) (2)	Operating Speed (km/h)
Identi-fication	Name (Country)				
A12	ROSAN (USA)	SLIDER	SMOOTH	100	10
A13	DF TESTER (J)	SLIDER	SMOOTH	100	0-80
A14	BRITISH PENDULUM (CH)	SLIDER	SMOOTH	100	10
B1-ABS	STUTTGARTER REIBUNGSMESSER (CH)	OPTIMUM SLIP	RIBBED P	OPT.	30,60,90
B1-LKD	STUTTGARTER REIBUNGSMESSER (CH)	LOCKED WHEEL	RIBBED P	100	30,60,90
B1-SLP	STUTTGARTER REIBUNGSMESSER (CH)	FIXED SLIP	RIBBED P	14	30,60,90
B2-LKD	SKIDDOMETER BV-8 (CH)	LOCKED WHEEL	RIBBED P	100	30,60,90
B2-SLP	SKIDDOMETER BV-8 (CH)	FIXED SLIP	RIBBED P	20	30,60,90
B3	SKIDDOMETER BV-11 (S)	FIXED SLIP	PATTERNED	20	30,60,90
B4E-SLP	NORSEMETER OSCAR (N)	FIXED SLIP	SMOOTH A	20	30,60,90
B4E-SWP	NORSEMETER OSCAR (N)	VARIABLE SLIP	SMOOTH A	0-90	30,60,90
B5-ABS	STUTTGARTER REIBUNGSMESSER (A)	OPTIMUM SLIP	RIBBED P	OPT.	30,60,90
B5-LKD	STUTTGARTER REIBUNGSMESSER (A)	LOCKED WHEEL	RIBBED P	100	30,60,90
B5-SLP	STUTTGARTER REIBUNGSMESSER (A)	FIXED SLIP	RIBBED P	20	30,60,90
B6-501	ASTM E-274 TRAILER (USA)	LOCKED WHEEL	RIBBED A	100	65
B6-524	ASTM E-274 TRAILER (USA)	LOCKED WHEEL	SMOOTH A	100	30,65,90
B6-CHP	ASTM E-274 TRAILER (USA)	DRY PEAK	PATTERNED	MAX.	65
B6-ULT	ASTM E-274 TRAILER (USA)	DRY LOCKED	SMOOTH A	100	10
B7	BRITISH PENDULUM (CH)	SLIDER	SMOOTH	100	10

(1) A = ASTM tyre ; P = PIARC tyre ; PATTERNED = Tyres with various tread patterns.
(2) For SFC devices the equivalent rate of slip is given, followed by the yaw angle in parenthesis.

(continued)

DEVICE		MEASUREMENT TYPE	TYRE TYPE (1)	RATE OF SLIP (%) (2)	Operating speed (km/h)
Identification	Name (Country)				
B10E	MuMETER (E)	SIDE FORCE	PATTERNED	13(7.5°)	80
C1	SKID RESISTANCE TESTER (P)	LOCKED WHEEL	PATTERNED	100	30,60,90
C3B	FLEMISH SCRIM (B)	SIDE FORCE	SMOOTH	34(20°)	30,60,90
C3E	CEDEX SCRIM (E)	SIDE FORCE	SMOOTH	34(20°)	30,60,90
C4	KOMATSU SKID TESTER (J)	VARIABLE SLIP	SMOOTH A	10-30	30,50,60
C5	DWW TRAILER (NL)	FIXED SLIP	SMOOTH P	86	30,50,90
C6E	MOPT SCRIM (E)	SIDE FORCE	SMOOTH	34(20°)	30,60,90
C8	STRADOGRAPH (DK)	SIDE FORCE	SMOOTH P	21(12°)	30,60,90
C9	WALLODN ODOLIOGRAPH (B)	SIDE FORCE	SMOOTH P	26(15°)	30,50,90
C10	CRR ODOLIOGRAPH (B)	SIDE FORCE	SMOOTH P	34(20°)	30,50,90
D1E	SCRIM (D)	SIDE FORCE	SMOOTH	34(20°)	40,60,90
D2	SCRIM GEOCISA (E)	SIDE FORCE	SMOOTH	34(20°)	30,60,80
D3	SCRIM (F)	SIDE FORCE	SMOOTH	34(20°)	30,60,90
D4	SUMMS (I)	SIDE FORCE	SMOOTH	34(20°)	50,60,80
D5	SCRIMTEX (GB)	SIDE FORCE	SMOOTH	34(20°)	30,50,90
D6	ADHERA LCPC (F)	LOCKED WHEEL	SMOOTH P	100	40,60,90
D7B	PETRA (D)	VARIABLE SLIP	PATTERNED	0-100	30,60,90
D8	GRIPTESTER (GB)	FIXED SLIP	SMOOTH	18	5,30,65,90

(1) A = ASTM tyre ; P = PIARC tyre ; PATTERNED = Tyres with various tread patterns.
(2) For SFC devices the equivalent rate of slip is given, followed by the yaw angle in parenthesis.

Table 2 - Texture devices participating in the PIARC experiment. The European devices selected for defining EFI are in grey tint blocks

DEVICE		MEASUREMENTS	SPEED
Identification	Name (Country)		(km/h)
A1	TEXTURE VAN de la FHWA (USA)	RMS	30
A2	PROFILOMETRE MOBILE du VTI (S)	RMS, ETD, TDMA, MPD	36
A3B	ARAN-Automated Road Analyzer (CDN)	MPD, RMS	30,60,80
A3E	RST-Road Surface Tester AEPO (F)	MACRO-, MEGA-TEXTURE	30
A4	PROFILOMETRE MOBILE du CRR (B)	MPD, RMS	18,36,72
A5	PROFILOMETRE STATIONNAIRE du CRR (B)	MPD, RMS, ISO	0
A8	TACHE DE SABLE ASTM E-965 (USA)	MTD	0
A12	ROSAN de la FHWA (USA)	Calculated MTD	5
B8	DRAINOMETRE (CH)	Time of water outflow	0
B11E	DRAINOMETRE (USA)	Time of water outflow	0
D2	SCRIM de GEOCISA (E)	Calculated MTD	60
D3	RUGOLASER (F)	RA, RQ, HSC	60
D4	SUMMS (I)	Calculated MTD	50
D5	SCRIMTEX (GB)	Calculated MTD	50

Table 3 - Comparison between the MPD values determined in the PIARC experiment using the CRR processing method and the MPD values calculated from the same data using the ISO standard method issued at a later date

SITE	A5/MPD	A5/ISO
1A	2.82	2.27
1B	3,46	2,78
2A	1,42	1,17
2B	1,27	1,14
3A	0,88	0,72
3B	1,05	0,82
4A	0,89	0,74
4B	1,02	0,81
6A	0,75	0,59
6B	0,84	0,65
8A	0,57	0,49
8B	0,53	0,46
9A	2,19	1,66
9B	1,44	1,14
10A	2,11	1,68
10B	1,62	1,22
11A	1,00	0,82
11B	0,85	0,67
12A	2,66	2,11
12B	2,76	2,15
13A	3,04	2,36
13B	3,75	3,10
15A	3,58	2,80
15B	3,72	2,82
17A	1,02	0,76
17B	1,92	1,40
18A	1,99	1,70
18B	1,84	1,47
19A	3,25	2,57
19B	4,00	3,01
21A	1,76	1,45
21B	1,90	1,56
24A	1,28	0,96
24B	1,17	0,97
26,1A	0,55	0,48
26,1B	0,55	0,50
26,2A	2,08	1,90
26,2B	2,39	2,12
32A	1,94	1,65
32B	1,79	1,37
33,1	0,63	0,53
33,2	0,70	0,57
33,3	0,79	0,64
33,4	0,78	0,60
34A	1,24	1,10
34B	1,15	0,98
40A	1,39	1,14
40B	1,31	1,06
41A	1,61	1,41
41B	1,73	1,55

SITE	A5/MPD	A5/ISO
42A	0.72	0.59
42B	0,73	0,61
50A	0,73	0,60
50B	0,96	0,76
51A	0,78	0,64
51B	1,05	0,79
52A	0,86	0,70
52B	0,88	0,72
53A	0,65	0,54
53B	0,77	0,64
56A	1,12	0,97
56B	0,89	0,80
57A	2,54	2,10
57B	2,85	2,25
58A	1,23	0,96
58B	1,46	1,07
59A	0,95	0,76
59B	0,87	0,74
60A	0,87	0,65
60B	0,81	0,64
61A	0,72	0,53
61B	0,59	0,48
62A	1,64	1,50
62B	1,84	1,43
63A	1,88	1,56
63B	2,36	2,04
64A	3,35	2,45
64B	1,74	1,41
65A	0,83	0,62
65B	0,87	0,72
66A	0,77	0,60
66B	0,74	0,62
67A	1,23	1,03
67B	1,38	1,17
68A	0,93	0,70
68B	0,89	0,72
69A	0,71	0,55
69B	0,71	0,62
70A	2,01	1,68
70B	2,12	1,80
81,1A	0,49	0,44
81,1B	0,55	0,47
81,2A	0,61	0,54
81,2B	0,51	0,45
81,3A	0,60	0,52
81,3B	0,60	0,53
81,4A	0,59	0,50
81,4B	0,66	0,57
82,1	1,21	1,06
82,2	0,87	0,78
82,3	0,99	0,79

Table 4 - Parameters of the linear regression $S_{oj}^* = A_{ISO} + B_{ISO} * T_{ISO}$.

	All tyres	Smooth tyres	Patterned tyres
a [km/h]	57	31	85
b [km/h/mm]	56	71	42
ρ	0,88	0,86	0,82
σ abs [km/h]	20	29	20
σ rel [%]	17	24	16

Table 5 - Parameters of the regressions enabling each defice to predict EFI.

Device	n	A	B	ρ	σ_{abs}	σ_{rel}
B1LKD	318	0,1814	0,5896	0,7940	0,0656	0,1143
B1SLP	339	0,1443	0,6666	0,8205	0,0610	0,1185
B2LKD	261	0,3470	0,3402	0,5967	0,0831	0,1453
B2SLP	234	0,0867	0,8420	0,9069	0,0369	0,0717
B3	524	0,1006	0,7798	0,9044	0,0431	0,0793
B5LKD	479	0,1407	0,6837	0,7762	0,0651	0,1167
B5SLP	512	0,0379	0,8946	0,8984	0,0434	0,0786
C1	464	0,1037	0,8859	0,8271	0,0582	0,1062
C3B	252	0,0604	1,0114	0,9321	0,0318	0,0568
C5	526	0,1002	0,7511	0,8634	0,0498	0,0867
C6E	181	0,1145	0,8152	0,8944	0,0372	0,0750
C8	530	0,1712	0,6515	0,8545	0,0491	0,0918
C9	562	0,2908	0,5136	0,7808	0,0563	0,1178
C10	498	0,2585	0,5743	0,8243	0,0551	0,1120
D1E	204	0,1170	0,7538	0,9293	0,0320	0,0604
D2	460	0,1213	0,7912	0,8353	0,0468	0,0882
D3	500	0,0668	0,7910	0,8978	0,0387	0,0759
D4	519	0,0265	1,0165	0,8692	0,0470	0,0865
D5	499	0,0063	0,9917	0,8767	0,0451	0,0813
D6	492	0,2034	0,7000	0,8691	0,0471	0,0959
D8	610	0,1901	0,7792	0,8231	0,0490	0,0971
B1LKD_RP	318	0,1448	0,7104	0,8953	0,0479	0,0849
B1SLP_RP	339	0,1527	0,6894	0,8379	0,0589	0,1120
B2LKD_RP	261	0,2907	0,4947	0,7859	0,0636	0,1059
B2SLP_RP	234	0,1228	0,8190	0,8605	0,0450	0,0797
B3_RP	524	0,1361	0,7573	0,8870	0,0459	0,0791
B5LKD_RP	479	0,1028	0,8131	0,8930	0,0447	0,0792
B5SLP_RP	512	0,0755	0,8652	0,8761	0,0471	0,0813
C1_RP	464	0,0931	0,9846	0,8845	0,0481	0,0852
C3B_B	252	0,0344	1,0360	0,9307	0,0329	0,0609
C5_B	526	0,1601	0,6044	0,7363	0,0673	0,1206
C6E_B	181	0,0783	0,8556	0,9165	0,0350	0,0743
C8_B	530	0,1335	0,6938	0,8857	0,0458	0,0882
C9_B	562	0,2466	0,5715	0,8400	0,0513	0,1141
C10_B	498	0,2158	0,6258	0,8642	0,0509	0,1097
D1E_B	204	0,0792	0,7984	0,9426	0,0307	0,0606
D2_B	460	0,0813	0,8377	0,8555	0,0455	0,0887
D3'B	500	0,0337	0,8218	0,8931	0,0413	0,0852
D4_B	519	0,0123	1,0112	0,8927	0,0426	0,0843
D5_B	499	-0,0137	0,9999	0,9103	0,0385	0,0741
D6_B	492	0,1077	0,8308	0,8985	0,0442	0,0909
D8_B	610	0,1605	0,8117	0,8634	0,0440	0,0907

Table 6 - Repeatability, r_j, and reproducibility, R_j, of EFI per half site j

	Trimmed data				Untrimmed data			
Tyres	Without distinction		Distinction B & RP		Without distinction		Distinction B & RP	
Site	*rj*	*Rj*	*rj*	*Rj*	*rj*	*Rj*	*rj*	*Rj*
1A	0,056	0,085	0,056	0,077	0,056	0,085	0,056	0,077
1B	0,062	0,100	0,065	0,094	0,062	0,100	0,065	0,094
2A	0,065	0,131	0,067	0,111	0,065	0,131	0,067	0,111
2B	0,063	0,101	0,065	0,082	0,063	0,101	0,065	0,082
4A	0,097	0,142	0,094	0,139	0,097	0,142	0,094	0,139
4B	0,102	0,140	0,102	0,139	0,102	0,140	0,102	0,139
6A	0,087	0,149	0,091	0,135	0,087	0,149	0,091	0,135
6B	0,096	0,124	0,103	0,116	0,096	0,124	0,103	0,116
8A	0,131	0,252	0,137	0,223	0,131	0,252	0,137	0,223
8B	0,140	0,282	0,146	0,249	0,140	0,282	0,146	0,249
9A	0,048	0,056	0,048	0,053	0,048	0,056	0,048	0,053
9B	0,058	0,122	0,059	0,116	0,058	0,122	0,059	0,116
10A	0,083	0,161	0,087	0,150	0,083	0,161	0,087	0,150
10B	0,095	0,116	0,104	0,119	0,095	0,116	0,104	0,119
11A	0,106	0,229	0,107	0,232	0,106	0,229	0,107	0,232
11B	0,104	0,257	0,093	0,251	0,104	0,257	0,093	0,251
12A	0,070	0,070	0,072	0,072	0,075	0,075	0,077	0,077
12B	0,076	0,076	0,078	0,078	0,075	0,081	0,079	0,090
13A	0,054	0,104	0,055	0,097	0,054	0,099	0,056	0,096
13B	0,066	0,069	0,071	0,071	0,066	0,069	0,071	0,071
15A	0,058	0,118	0,060	0,116	0,058	0,118	0,060	0,116
15B	0,054	0,131	0,057	0,139	0,057	0,128	0,061	0,128
17A	0,092	0,092	0,095	0,123	0,092	0,092	0,095	0,123
17B	0,089	0,107	0,093	0,123	0,095	0,112	0,102	0,137
18A	0,054	0,090	0,055	0,085	0,054	0,087	0,055	0,085
18B	0,055	0,055	0,053	0,053	0,055	0,070	0,054	0,068
19A	0,053	0,053	0,055	0,055	0,054	0,066	0,055	0,062
19B	0,050	0,050	0,051	0,051	0,049	0,099	0,051	0,092
21A	0,054	0,054	0,054	0,054	0,054	0,054	0,055	0,061
21B	0,046	0,046	0,046	0,047	0,047	0,047	0,047	0,049
24A	0,052	0,087	0,053	0,053	0,072	0,098	0,073	0,073
24B	0,048	0,093	0,052	0,052	0,063	0,098	0,067	0,067
26,1A	0,141	0,141	0,112	0,112	0,175	0,175	0,163	0,163
26,1B	0,139	0,139	0,110	0,110	0,171	0,171	0,154	0,154
26,2A	0,083	0,083	0,086	0,086	0,087	0,087	0,089	0,089
26,2B	0,080	0,080	0,084	0,084	0,079	0,079	0,082	0,082
32A	0,059	0,121	0,060	0,120	0,059	0,121	0,060	0,120
32B	0,061	0,095	0,061	0,090	0,061	0,095	0,061	0,090
33,1A	0,132	0,390	0,119	0,382	0,135	0,363	0,123	0,352
33,1B	0,113	0,418	0,099	0,412	0,122	0,391	0,110	0,383
33,2A	0,091	0,242	0,084	0,182	0,091	0,236	0,088	0,173
33,2B	0,095	0,119	0,090	0,090	0,095	0,119	0,090	0,090
33,3A	0,115	0,201	0,117	0,194	0,118	0,197	0,121	0,184
33,3B	0,118	0,196	0,119	0,180	0,121	0,198	0,123	0,187
33,4A	0,100	0,285	0,102	0,270	0,097	0,260	0,101	0,231
33,4B	0,101	0,248	0,101	0,217	0,101	0,248	0,101	0,217

Tyres	Trimmed data				Untrimmed data			
	Without distinction		Distinction B & RP		Without distinction		Distinction B & RP	
Site	*rj*	*Rj*	*rj*	*Rj*	*rj*	*Rj*	*rj*	*Rj*
34A					0,104	0,105	0,109	0,109
34B					0,102	0,110	0,111	0,111
40A	0,064	0,064	0,066	0,066	0,063	0,064	0,065	0,065
40B	0,067	0,077	0,071	0,076	0,067	0,077	0,071	0,076
41A	0,095	0,095	0,095	0,095	0,093	0,093	0,093	0,093
41B	0,105	0,105	0,106	0,106	0,102	0,102	0,103	0,103
42A	0,099	0,197	0,101	0,162	0,099	0,197	0,101	0,162
42B	0,099	0,219	0,105	0,189	0,099	0,219	0,105	0,189
50A	0,100	0,216	0,099	0,185	0,118	0,197	0,118	0,165
50B	0,106	0,201	0,102	0,174	0,133	0,190	0,132	0,166
51A	0,076	0,154	0,074	0,125	0,076	0,154	0,074	0,125
51B	0,069	0,096	0,069	0,077	0,069	0,096	0,069	0,077
52A	0,069	0,129	0,068	0,101	0,069	0,129	0,068	0,101
52B	0,070	0,114	0,070	0,087	0,070	0,114	0,070	0,087
53A	0,133	0,313	0,125	0,288	0,130	0,300	0,125	0,278
53B	0,145	0,269	0,140	0,247	0,145	0,269	0,140	0,247
56A	0,073	0,181	0,074	0,162	0,073	0,181	0,074	0,162
56B	0,096	0,212	0,096	0,192	0,096	0,212	0,096	0,192
57A	0,050	0,118	0,053	0,132	0,050	0,118	0,053	0,132
57B	0,048	0,086	0,050	0,100	0,048	0,086	0,050	0,100
58A	0,065	0,345	0,066	0,340	0,065	0,345	0,066	0,340
58B	0,070	0,345	0,070	0,345	0,069	0,329	0,070	0,326
59A	0,087	0,191	0,086	0,162	0,087	0,191	0,086	0,162
59B	0,094	0,167	0,094	0,140	0,094	0,167	0,094	0,140
60A	0,083	0,116	0,083	0,089	0,083	0,116	0,083	0,089
60B	0,082	0,113	0,085	0,090	0,082	0,113	0,085	0,090
61A	0,124	0,126	0,120	0,120	0,122	0,128	0,117	0,117
61B	0,139	0,173	0,134	0,136	0,135	0,178	0,131	0,142
62A	0,055	0,210	0,057	0,216	0,063	0,222	0,065	0,221
62B	0,063	0,191	0,066	0,190	0,067	0,198	0,070	0,195
63A	0,064	0,064	0,065	0,065	0,061	0,106	0,062	0,092
63B	0,057	0,057	0,059	0,059	0,058	0,067	0,061	0,061
64A	0,048	0,229	0,051	0,251	0,046	0,206	0,049	0,220
64B	0,056	0,172	0,058	0,181	0,056	0,172	0,058	0,181
65A	0,070	0,070	0,068	0,083	0,070	0,070	0,068	0,083
65B	0,075	0,093	0,076	0,115	0,075	0,093	0,076	0,115
66A	0,067	0,134	0,060	0,094	0,072	0,171	0,074	0,132
66B	0,075	0,146	0,071	0,108	0,081	0,183	0,084	0,145
67A	0,095	0,095	0,098	0,098	0,095	0,095	0,098	0,098
67B	0,064	0,064	0,066	0,066	0,064	0,064	0,066	0,066
68A	0,065	0,182	0,070	0,150	0,094	0,194	0,100	0,163
68B	0,067	0,130	0,072	0,100	0,067	0,130	0,072	0,100
69A	0,090	0,139	0,086	0,110	0,090	0,139	0,086	0,110
69B	0,079	0,166	0,078	0,142	0,079	0,166	0,078	0,142
70A	0,072	0,086	0,075	0,088	0,072	0,086	0,075	0,088
70B	0,076	0,083	0,079	0,085	0,076	0,083	0,079	0,085

	Trimmed data				Untrimmed data			
Tyres	Without distinction		Distinction B & RP		Without distinction		Distinction B & RP	
Site	*ηj*	*Rj*	*ηj*	*Rj*	*ηj*	*Rj*	*ηj*	*Rj*
81,1A					0,272	0,393	0,272	0,354
81,1B					0,272	0,411	0,272	0,338
81,2A					0,271	0,316	0,260	0,285
81,2B					0,279	0,412	0,275	0,337
81,3A					0,284	0,487	0,262	0,475
81,3B					0,295	0,560	0,275	0,533
81,4A					0,298	0,460	0,283	0,451
81,4B					0,290	0,499	0,274	0,478
82,1A	0,103	0,182	0,110	0,198	0,112	0,204	0,116	0,228
82,1B	0,111	0,215	0,108	0,223	0,111	0,215	0,108	0,223
82,2A					0,169	0,169	0,156	0,156
82,2B					0,168	0,168	0,155	0,155
82,3A	0,119	0,128	0,118	0,142	0,169	0,176	0,159	0,181
82,3B	0,133	0,133	0,136	0,136	0,187	0,226	0,178	0,228
Average :	0,083	0,148	0,083	0,138	0,103	0,173	0,103	0,161

Table 7 - Sites for the additional measurements in Belgium.

No. of site	No. of road	Place	Direction	Section Start mark - end mark	Type of surfacing (2)
1	N40	Neupont	Neufchâteau	71.050-70.900	E
2	N947	Dave	Namur	4.600-4.450	BB
3	N495	Geraardsberg	Edingen	2.550-2.700	BB
4	N437	Kruishoutem	Kruishoutem	29.300-29.150	BB
5	N7	Saintes	Halle	5.100-5.300	BC
6	N368	Eernegem	Ichtegem	0.800-0.650	BC
7	N255	Herne	Ninove	6.700-6.850	SMA
8	N255	Herne	Ninove	6.400-6.550	SMA
9	N255	Herne	Ninove	6.000-6.150	BD
10	N255	Herne	Ninove	5.300-5.450	ED
11	N255	Herne	Ninove	4.350-4.500	BC
12	N255	Herne	Ninove	4.000-4.150	BB
13	E411	Beez (viaduc)	Bruxelles	55.800-55.650	ESHP
14	N951	Wépion	Meuse	1.500-1.350	RMTO
15	N90	Floreffe (1)	Charleroi	62.900-62.750	RMTO
16	N5	Fraire	Charleroi	68.800-68.650	ED
17	N5	Philippeville	Couvin	76.400-76.550	BC
18	N5	Couvin	Couvin	91.400-91.550	RMD
19	N99	Couvin	Chimay	26.000-26.150	ED
20	N7	Leuze	Bruxelles	48.700-48.550	RMD
21	N526	Tourpes	Beloeil	4.800-4.950	RUMG
22	N25	Leuven	Namur	1.100-1.250	BC
23	N264	Leuven	Bruxelles	0.200-1.000	BC
24	R23	Leuven	Bruxelles	03.00-0.450	RMTO
25	N264	Leuven (1)	Bruxelles	0.000-0.150	SMA

(1) Impracticable at the time of testing.
(2) Code: E = Dressing, BB = Asphalt, BC = Aggregate concrete, ED = Porous asphalt, SMA = Stone Mastix Asphalt, RUMG = Coarse-graded ultrathin surfacing, RMTO = Open-textured thin surfacing, ESHP = High-performance surface dressing, RMD = Gap-graded thin surfacing. More Detailed descriptions can be found in **Appendix 1**.

Table 8 - Results of the additional measurements in Belgium with the SCRIM of LIN

Half-section	T_{ISO} (mm)	S_o (kmph)	F_o	F_{10}	F_{20}	F_{30}
1A	1,73	119,054	0,903	0,830	0,763	0,702
1B	1,48	118,149	0,862	0,792	0,727	0,668
2A	0,74	75,366	0,865	0,758	0,664	0,581
2B	0,70	65,113	0,895	0,767	0,658	0,564
3A	0,82	78,664	0,695	0,612	0,539	0,475
3B	1,07	68,948	0,748	0,647	0,560	0,484
4A	0,58	75,153	0,734	0,643	0,563	0,493
4B	0,68	66,509	0,753	0,648	0,558	0,480
5A	1,06	90,758	0,804	0,720	0,645	0,578
5B	1,24	100,097	0,803	0,727	0,658	0,595
6A	1,30	108,857	0,687	0,627	0,572	0,522
6B	1,32	98,495	0,700	0,633	0,572	0,516
7A	0,99	107,365	0,775	0,706	0,644	0,586
7B	1,01	86,526	0,793	0,707	0,629	0,561
8A	0,96	54,983	0,926	0,772	0,643	0,536
8B	1,08	56,767	0,936	0,785	0,658	0,552
9A	1,75	100,305	0,644	0,583	0,528	0,478
9B	1,44	102,328	0,613	0,556	0,504	0,458
10A	1,54	67,919	0,763	0,659	0,568	0,491
10B	1,72	67,573	0,791	0,682	0,588	0,507
11A	0,78	94,295	0,735	0,661	0,594	0,534
11B	0,71	81,906	0,730	0,646	0,572	0,506
12A	0,87	56,031	0,909	0,760	0,636	0,532
12B	0,78	50,851	0,919	0,755	0,620	0,509
13A	1,09	147,691	0,920	0,860	0,803	0,751
13B	1,12	164,855	0,921	0,867	0,816	0,768
14B	1,53	41,309	0,831	0,652	0,512	0,402
16A	2,33	95,066	0,607	0,546	0,492	0,443
16B	2,62	108,905	0,607	0,554	0,505	0,461
17A	0,60	85,180	0,768	0,682	0,607	0,540
17B	0,53	53,353	0,783	0,649	0,538	0,446
18A	1,08	113,516	0,617	0,565	0,517	0,474
18B	0,97	118,524	0,622	0,571	0,525	0,483
19A	1,80	89,588	0,642	0,574	0,514	0,459
19B	1,90	98,038	0,629	0,568	0,513	0,464
20A	1,00	122,755	0,522	0,482	0,444	0,409
20B	1,10	133,966	0,509	0,472	0,438	0,407
21A	1,32	108,535	0,623	0,568	0,518	0,472
21B	1,00	122,190	0,612	0,564	0,519	0,479
22A	2,10	108,036	0,704	0,642	0,585	0,533
22B	2,10	105,299	0,701	0,637	0,580	0,527
23A	1,16	90,589	0,658	0,589	0,528	0,473
23B	1,00	78,315	0,686	0,604	0,532	0,468
24A	1,68	91,463	0,537	0,481	0,431	0,387
24B	1,55	73,987	0,573	0,500	0,437	0,382

Table 9 - Results of the additional measurements in Belgium with the odoliograph of CRR.

Half-section	T_{ISO} (mm)	S_o (kmph)	F_o	F_{10}	F_{20}	F_{30}
1A	1,73	87	0,910	0,812	0,724	0,646
1B	1,48	238	0,863	0,827	0,793	0,761
2A	0,74	106	0,888	0,809	0,736	0,671
2B	0,70	71	0,960	0,834	0,724	0,629
3A	0,82	62	0,759	0,646	0,550	0,468
3B	1,07	56	0,782	0,655	0,548	0,459
4A	0,58	52	0,838	0,692	0,571	0,472
4B	0,68	49	0,845	0,690	0,563	0,460
5A	1,06	181	0,794	0,752	0,711	0,673
5B	1,24	433	0,770	0,753	0,735	0,719
6A	1,30	98	0,674	0,609	0,550	0,497
6B	1,32	103	0,657	0,596	0,542	0,492
7A	0,99	295	0,762	0,736	0,712	0,688
7B	1,01	203	0,794	0,756	0,720	0,685
8A	0,96	377	0,738	0,718	0,700	0,681
8B	1,08	348	0,756	0,734	0,714	0,693
9A	1,75	365	0,610	0,593	0,577	0,562
9B	1,44	277	0,580	0,559	0,539	0,520
10A	1,54	103	0,706	0,641	0,582	0,528
10B	1,72	135	0,704	0,654	0,607	0,564
11A	0,78	185	0,735	0,696	0,659	0,625
12A	0,87	88	0,864	0,771	0,688	0,614
12B	0,78	85	0,815	0,725	0,645	0,574
13A	1,09	33	1,009	0,743	0,548	0,404
13B	1,12	29	1,115	0,791	0,561	0,398
14A	1,46	105	0,849	0,772	0,701	0,638
14B	1,53	69	0,907	0,785	0,679	0,587
16A	2,33	56	0,727	0,608	0,508	0,425
16B	2,62	87	0,650	0,580	0,517	0,461
17A	0,60	72	0,814	0,709	0,617	0,537
17B	0,53	59	0,787	0,665	0,562	0,475
18A	1,08	153	0,716	0,671	0,628	0,589
18B	0,97	169	0,701	0,661	0,623	0,587
19A	1,80	64	0,729	0,624	0,534	0,456
19B	1,90	63	0,721	0,616	0,526	0,449
20A	1,00	140	0,661	0,615	0,573	0,533
20B	1,10	499	0,585	0,573	0,562	0,551
21A	1,32	88	0,667	0,596	0,532	0,475
21B	1,00	87	0,697	0,622	0,554	0,494
22A	2,10	135	0,708	0,657	0,610	0,567
22B	2,10	72	0,740	0,644	0,560	0,487
23A	1,16	130	0,612	0,567	0,525	0,486
23B	1,00	73	0,676	0,590	0,514	0,448
24A	1,68	125	0,515	0,476	0,439	0,405
24B	1,55	95	0,531	0,478	0,430	0,387

Table 10 - Standard deviation of the error in EFI due to imprecision in predicting S_p from texture with S_p = 50 kmph, which corresponds with MTD≅0.0 mm (absence of macrotexture).

S (kmph)	10	20	30	40	50	60	70	80	90
EFI									
0,1	0,02	0,01	0,00	0,01	0,02	0,02	0,03	0,04	0,05
0,2	0,03	0,02	0,00	0,02	0,03	0,05	0,06	0,08	0,10
0,3	0,05	0,02	0,00	0,02	0,05	0,07	0,10	0,12	0,14
0,4	0,06	0,03	0,00	0,03	0,06	0,10	0,13	0,16	0,19
0,5	0,08	0,04	0,00	0,04	0,08	0,12	0,16	0,20	0,24
0,6	0,10	0,05	0,00	0,05	0,10	0,14	0,19	0,24	0,29
0,7	0,11	0,06	0,00	0,06	0,11	0,17	0,22	0,28	0,34
0,8	0,13	0,06	0,00	0,06	0,13	0,19	0,26	0,32	0,38
0,9	0,14	0,07	0,00	0,07	0,14	0,22	0,29	0,36	0,43
1	0,16	0,08	0,00	0,08	0,16	0,24	0,32	0,40	0,48

Table 11 - Standard deviation of the error in EFI due to imprecision in predicting S_p from texture with S_p = 75 kmph, which corresponds with MTD≅0.3 mm.

S (kmph)	10	20	30	40	50	60	70	80	90
EFI									
0,1	0,01	0,00	0,00	0,00	0,01	0,01	0,01	0,02	0,02
0,2	0,01	0,01	0,00	0,01	0,01	0,02	0,03	0,04	0,04
0,3	0,02	0,01	0,00	0,01	0,02	0,03	0,04	0,05	0,06
0,4	0,03	0,01	0,00	0,01	0,03	0,04	0,06	0,07	0,09
0,5	0,04	0,02	0,00	0,02	0,04	0,05	0,07	0,09	0,11
0,6	0,04	0,02	0,00	0,02	0,04	0,06	0,09	0,11	0,13
0,7	0,05	0,02	0,00	0,02	0,05	0,07	0,10	0,12	0,15
0,8	0,06	0,03	0,00	0,03	0,06	0,09	0,11	0,14	0,17
0,9	0,06	0,03	0,00	0,03	0,06	0,10	0,13	0,16	0,19
1	0,07	0,04	0,00	0,04	0,07	0,11	0,14	0,18	0,21

Table 12- Standard deviation of the error in EFI due to imprecision in predicting S_p from texture with S_p = 100 kmph, which corresponds with MTD≅0.75 mm.

S (kmph)	10	20	30	40	50	60	70	80	90
EFI									
0,1	0,00	0,00	0,00	0,00	0,00	0,01	0,01	0,01	0,01
0,2	0,01	0,00	0,00	0,00	0,01	0,01	0,02	0,02	0,02
0,3	0,01	0,01	0,00	0,01	0,01	0,02	0,02	0,03	0,04
0,4	0,02	0,01	0,00	0,01	0,02	0,02	0,03	0,04	0,05
0,5	0,02	0,01	0,00	0,01	0,02	0,03	0,04	0,05	0,06
0,6	0,02	0,01	0,00	0,01	0,02	0,04	0,05	0,06	0,07
0,7	0,03	0,01	0,00	0,01	0,03	0,04	0,06	0,07	0,08
0,8	0,03	0,02	0,00	0,02	0,03	0,05	0,06	0,08	0,10
0,9	0,04	0,02	0,00	0,02	0,04	0,05	0,07	0,09	0,11
1	0,04	0,02	0,00	0,02	0,04	0,06	0,08	0,10	0,12

Table 13 - Standard deviation of the error in EFI due to imprecision in predicting S_p from texture with S_p = 150 kmph, which corresponds with MTD≅1.5 mm.

S (kmph)	10	20	30	40	50	60	70	80	90
EFI									
0,1	0,00	0,00	0,00	0,00	0,00	0,00	0,00	0,00	0,01
0,2	0,00	0,00	0,00	0,00	0,00	0,01	0,01	0,01	0,01
0,3	0,01	0,00	0,00	0,00	0,01	0,01	0,01	0,01	0,02
0,4	0,01	0,00	0,00	0,00	0,01	0,01	0,01	0,02	0,02
0,5	0,01	0,00	0,00	0,00	0,01	0,01	0,02	0,02	0,03
0,6	0,01	0,01	0,00	0,01	0,01	0,02	0,02	0,03	0,03
0,7	0,01	0,01	0,00	0,01	0,01	0,02	0,02	0,03	0,04
0,8	0,01	0,01	0,00	0,01	0,01	0,02	0,03	0,04	0,04
0,9	0,02	0,01	0,00	0,01	0,02	0,02	0,03	0,04	0,05
1	0,02	0,01	0,00	0,01	0,02	0,03	0,04	0,04	0,05

Table 14 - Standard deviation of the error in EFI due to imprecision in predicting S_p from texture with S_p = 200 kmph, which corresponds with MTD≅2.5 mm.

S (kmph)	10	20	30	40	50	60	70	80	90
EFI									
0,1	0,00	0,00	0,00	0,00	0,00	0,00	0,00	0,00	0,00
0,2	0,00	0,00	0,00	0,00	0,00	0,00	0,00	0,01	0,01
0,3	0,00	0,00	0,00	0,00	0,00	0,00	0,01	0,01	0,01
0,4	0,00	0,00	0,00	0,00	0,00	0,01	0,01	0,01	0,01
0,5	0,01	0,00	0,00	0,00	0,01	0,01	0,01	0,01	0,02
0,6	0,01	0,00	0,00	0,00	0,01	0,01	0,01	0,02	0,02
0,7	0,01	0,00	0,00	0,00	0,01	0,01	0,01	0,02	0,02
0,8	0,01	0,00	0,00	0,00	0,01	0,01	0,02	0,02	0,02
0,9	0,01	0,00	0,00	0,00	0,01	0,01	0,02	0,02	0,03
1	0,01	0,01	0,00	0,01	0,01	0,02	0,02	0,03	0,03

Table 15 - Standard deviation of the error in EFI dus to imprecision in predicting S_p from texture with S_p = 250 kmph, which corresponds with MTD≅3.5 mm.

S (kmph)	10	20	30	40	50	60	70	80	90
EFI									
0,1	0,00	0,00	0,00	0,00	0,00	0,00	0,00	0,00	0,00
0,2	0,00	0,00	0,00	0,00	0,00	0,00	0,00	0,00	0,00
0,3	0,00	0,00	0,00	0,00	0,00	0,00	0,00	0,00	0,01
0,4	0,00	0,00	0,00	0,00	0,00	0,00	0,01	0,01	0,01
0,5	0,00	0,00	0,00	0,00	0,00	0,00	0,01	0,01	0,01
0,6	0,00	0,00	0,00	0,00	0,00	0,01	0,01	0,01	0,01
0,7	0,00	0,00	0,00	0,00	0,00	0,01	0,01	0,01	0,01
0,8	0,01	0,00	0,00	0,00	0,01	0,01	0,01	0,01	0,02
0,9	0,01	0,00	0,00	0,00	0,01	0,01	0,01	0,01	0,02
1	0,01	0,00	0,00	0,00	0,01	0,01	0,01	0,02	0,02

XII. Figures

FIGURE 1 - EXAMPLE OF APPLICATION OF THE EXPONENTIAL MODEL TO A SERIES OF FRICTION MEASUREMENTS AT VARIOUS SPEEDS 48
FIGURE 2 - EXAMPLE OF DISCARDED OUTLYING SERIES 48
FIGURE 3 - RELATION BETWEEN MEAN TEXTURE DEPTH BY THE NEW ISO STANDARD AND BY THE BRRC METHOD 49
FIGURE 4 - EXAMPLE OF DETERMINATION OF THE OPTIMUM VALUE OF S_{oJ} (S_{oJ}*) - COMMON TO ALL DEVICES ON A GIVEN SITE (J) -, WHICH MINIMIZES THE RESIDUAL STANDARD DEVIATION OF THE MEASUREMENTS FROM THE EXPONENTIAL (REGRESSION) CURVES 50
FIGURE 5 - EXAMPLE OF THE FITTING OF EXPONENTIAL CURVES OF EQUAL SLOPE TO A SERIES OF DATA MEASURED WITH DIFFERENT DEVICES ON A GIVEN HALF SECTION 50
FIGURE 6 - EXAMPLE OF REGRESSION BETWEEN INDIVIDUAL FRICTION MEASUREMENTS REDUCED TO A COMMON REFERENCE SPEED (S_R = 40 KMPH) AND THE AVERAGE VALUE OF THESE MEASUREMENTS FOR ALL DEVICES ('GOLDEN VALUE') ON A GIVEN HALF SECTION 51
FIGURE 7 - RELATION $<F_R>_J$ VS F_{RMJ} OBTAINED ON A SITE, WITH A SERIES OF OUTLIERS 52
FIGURE 8 - ABSOLUTE AND RELATIVE RESIDUAL STANDARD DEVIATION OF FRICTION MEASUREMENTS FROM EXPONENTIAL CURVES OF EQUAL COMMON SLOPE PER SITE 52
FIGURE 9 - RELATION BETWEEN FITTED COMMON VALUES S_{oJ}* AND TEXTURE MEASUREMENT TISO FOR THE DEVICES WITH SMOOTH TYRES 53
FIGURE 10 - RELATION BETWEEN FITTED COMMON VALUES S_{oJ}* AND TEXTURE MEASUREMENT TISO FOR THE DEVICES WITH PATTERNED TYRES 53
FIGURE 11 - RELATION BETWEEN FITTED COMMON VALUES S_{oJ}* AND TEXTURE MEASUREMENT TISO FOR ALL DEVICES, REGARDLESS OF TYRE TYPE 54
FIGURE 12 - RELATION S_{oJ}* VS T_{ISO} TRIMMED OF OUTLIERS (SMOOTH TYRES) 54
FIGURE 13 - RELATION S_{oJ}* VS T_{ISO} TRIMMED OF OUTLIERS (PATTERNED TYRES) 55
FIGURE 14 - RELATION S_{oJ}* VS T_{ISO} TRIMMED OF OUTLIERS (ALL TYRES) 55
FIGURE 15 - STANDARD DEVIATION OF ERRORS IN EFI IF S_{oJ}* IS PREDICTED WITH A RANDOM ERROR, AS A FUNCTION OF THE REFERENCE SPEED CONSIDERED (SINGLE FORMULA FOR ALL TYRES TO PREDICT S_{oJ}* FROM T_{ISO}) 56
FIGURE 16 - STANDARD DEVIATION OF ERRORS IN EFI IF S_{oJ}* IS PREDICTED WITH A RANDOM ERROR, AS A FUNCTION OF THE REFERENCE SPEED CONSIDERED (DIFFERENT FORMULAS FOR THE TWO TYRE TYPES TO PREDICT S_{oJ}* FROM T_{ISO}) 56
FIGURE 17 - SERIES OF MEASUREMENTS SHOWING THAT THE FRICTION COEFFICIENT DEPENDS ON TWO INDEPENDENT VARIABLES: MEASURING SPEED AND SLIP ANGLE - AFTER W.B. HORNE, QUOTED BY Z. RADO [REF. 3] 57
FIGURE 18 - MODELS OF EQUATIONS FOR THE VARIATION OF THE FRICTION COEFFICIENT WITH SPEED (V), WITH THE SLIP ANGLE (τ), OR WITH BOTH 58
FIGURE 19 - THREE-DIMENSIONAL REPRESENTATION OF THE GENERAL MODEL 59
FIGURE 20 - APPLICATION OF THE GENERAL MODEL TO THE DATA OF **FIGURE 17** 60
FIGURE 21 - APPLICATION OF THE GENERAL MODEL TO THE DATA OF **FIGURE 17** 60
FIGURE 22 - APPLICATION OF THE GENERAL MODEL TO THE DATA OF **FIGURE 17** 61
FIGURE 23 - REPRESENTATION SUGGESTED BY H.W. KUMMER IN 1966 61
FIGURE 24 - COMPARISON OF S_{oIJ} VS T_{ISO} DIAGRAMS OBTAINED ON THE PIARC AND SSTC SITES USING THE SCRIM MEASUREMENTS 62
FIGURE 25 - COMPARISON OF S_{oIJ} VS T_{ISO} DIAGRAMS OBTAINED ON THE PIARC AND SSTC SITES USING THE ODOLIOGRAPH MEASUREMENTS 63
FIGURE 26 - DISTRIBUTION OF DIFFERENCES IN SFC VALUES PROVIDED BY THE SCRIM AND THE ODOLIOGRAPH MEASURING AT THE SAME SPEED ON THE SAME HALF SITE IN THE PIARC EXPERIMENT 64
FIGURE 27 - DISTRIBUTION OF DIFFERENCES IN EFI VALUES FOUND BY THE CONVERSION OF SCRIM AND ODOLIOGRAPH MEASUREMENTS IN THE PIARC EXPERIMENT 64
FIGURE 28 - DISTRIBUTION OF DIFFERENCES IN SFC VALUES PROVIDED BY THE SCRIM AND THE ODOLIOGRAPH TRAVELING AT THE SAME SPEED ON THE SAME HALF SITE IN THE 1997 MEASUREMENTS 65
FIGURE 29 - DISTRIBUTION OF DIFFERENCES IN EFI VALUES FOUND BY THE CONVERSION OF SCRIM AND ODOLIOGRAPH RESULTS IN THE 1997 EXPERIMENT 65

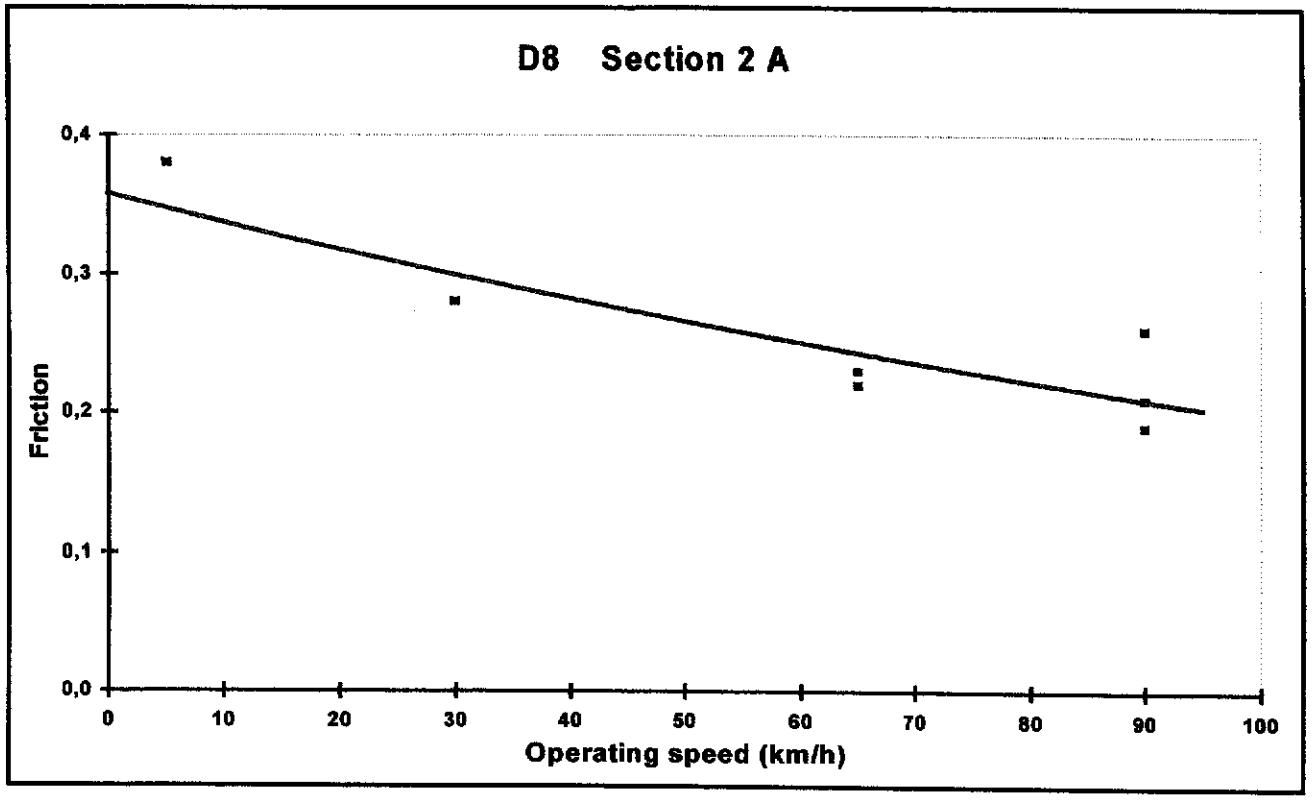

Figure 1 - Example of application of the exponential model to a series of friction measurements at various speeds

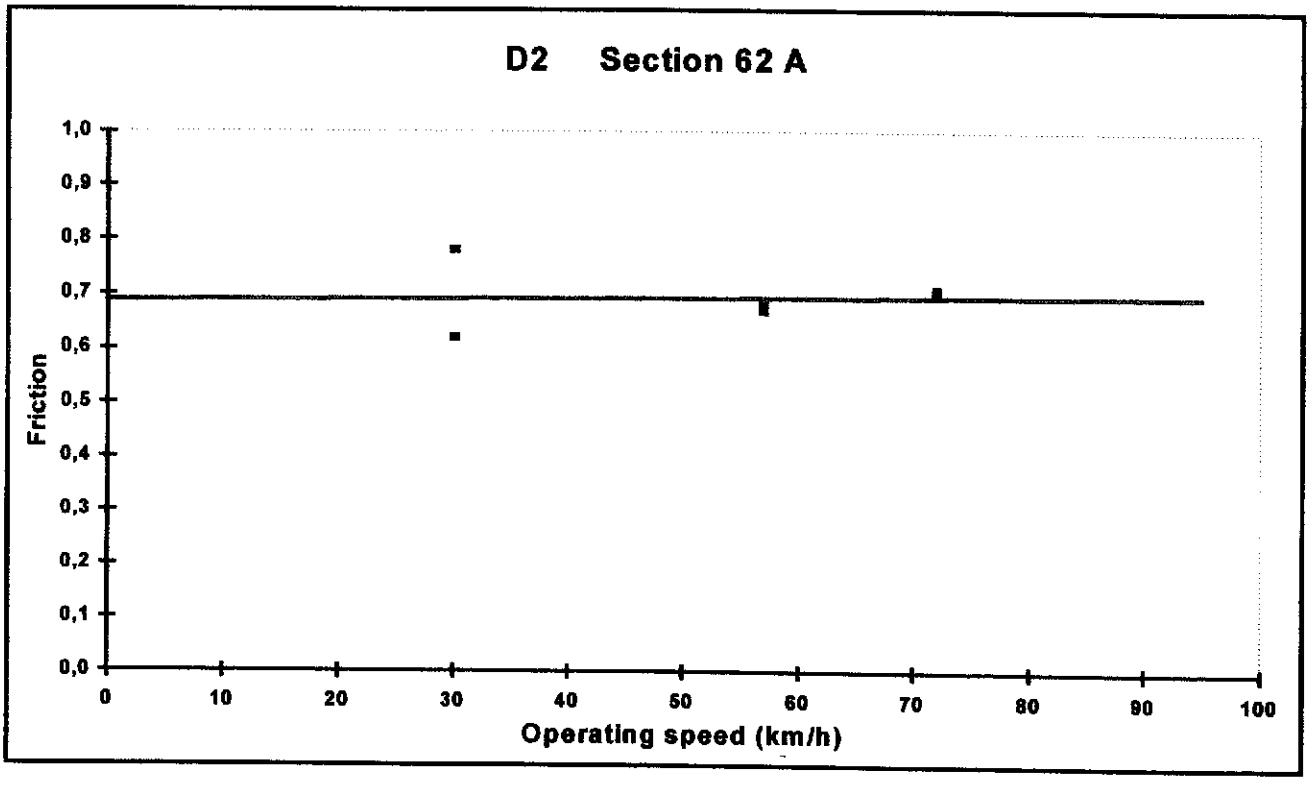

Figure 2 - Example of discarded outlying series

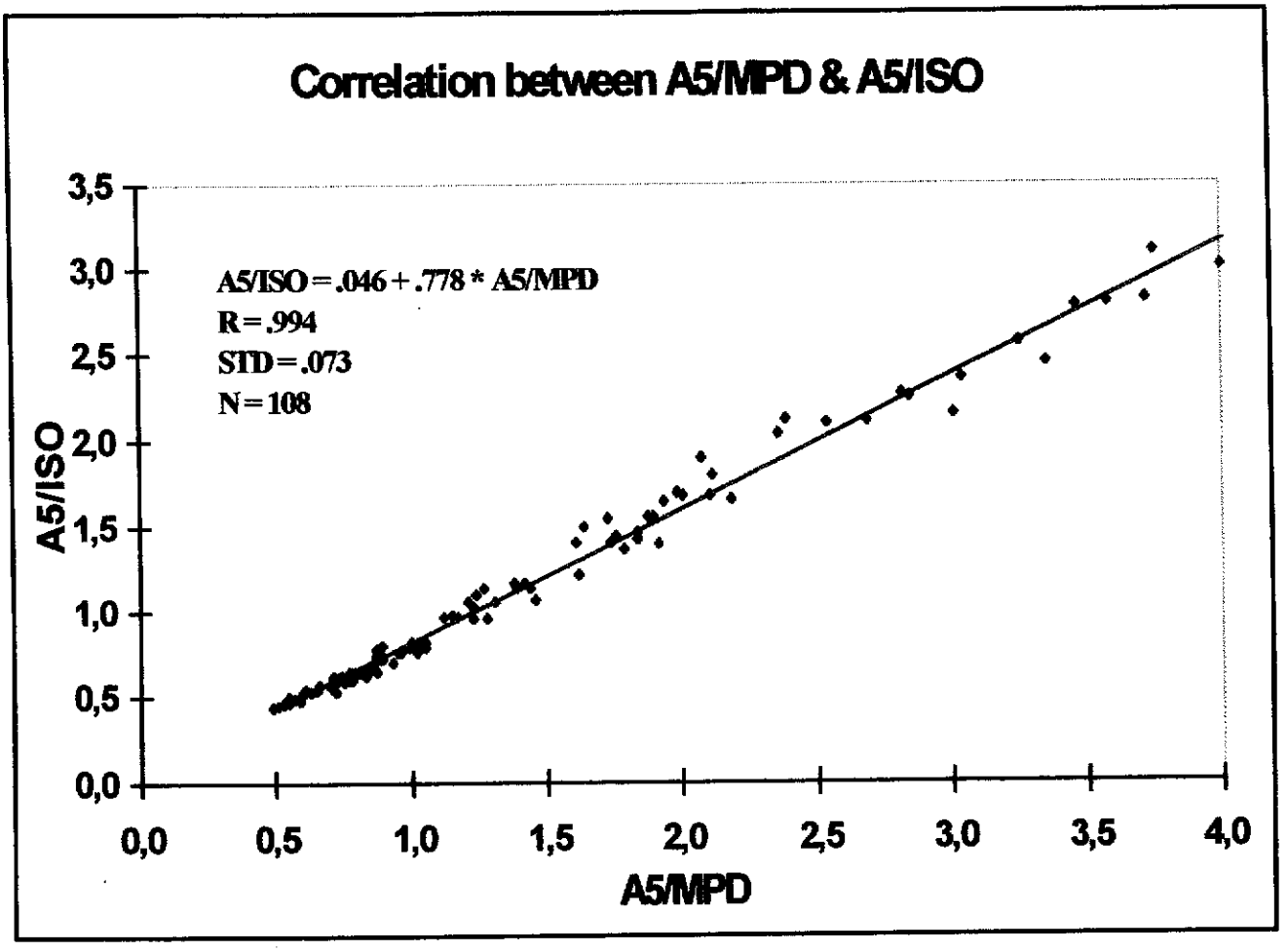

Figure 3 - Relation between mean texture depth by the new ISO standard and by the BRRC method

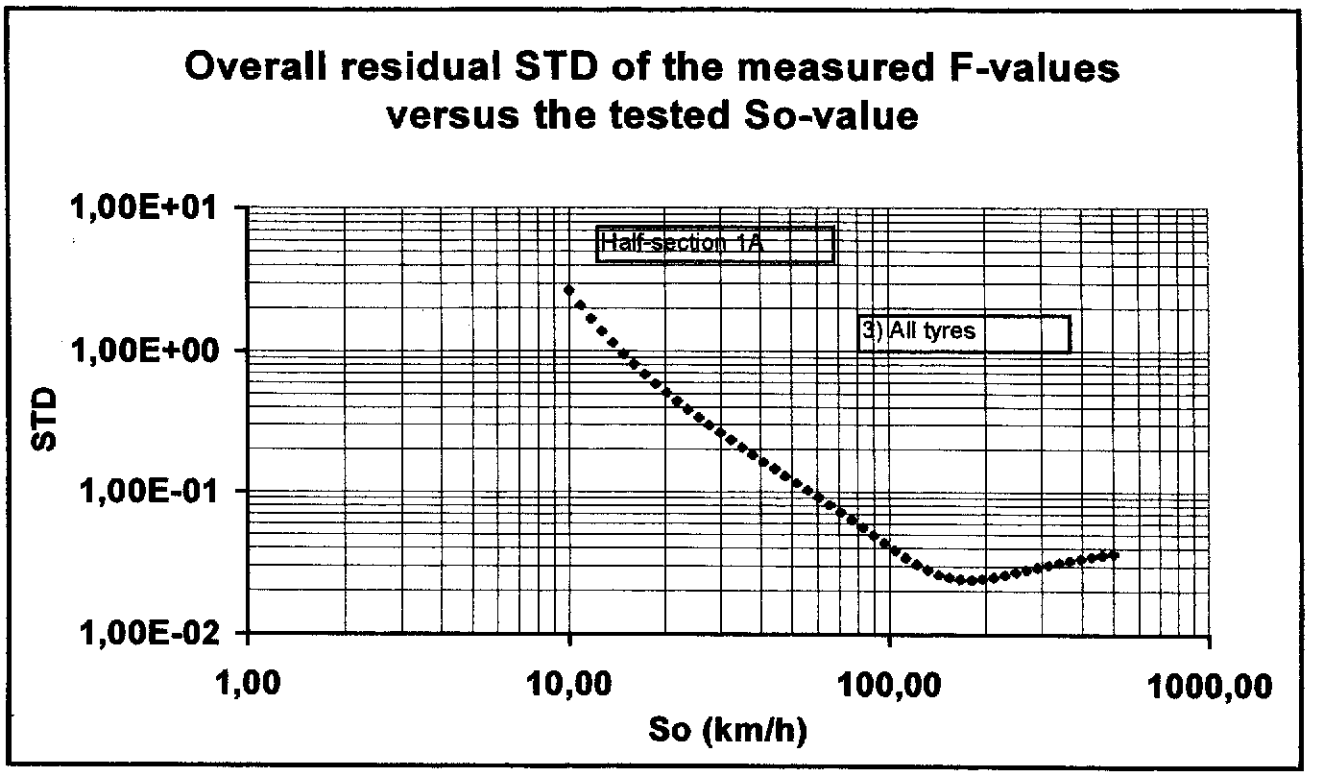

Figure 4 - Example of determination of the optimum value of S_{oj} (S_{oj}*) - common to all devices on a given site (j) -, which minimizes the residual standard deviation of the measurements from the exponential (regression) curves

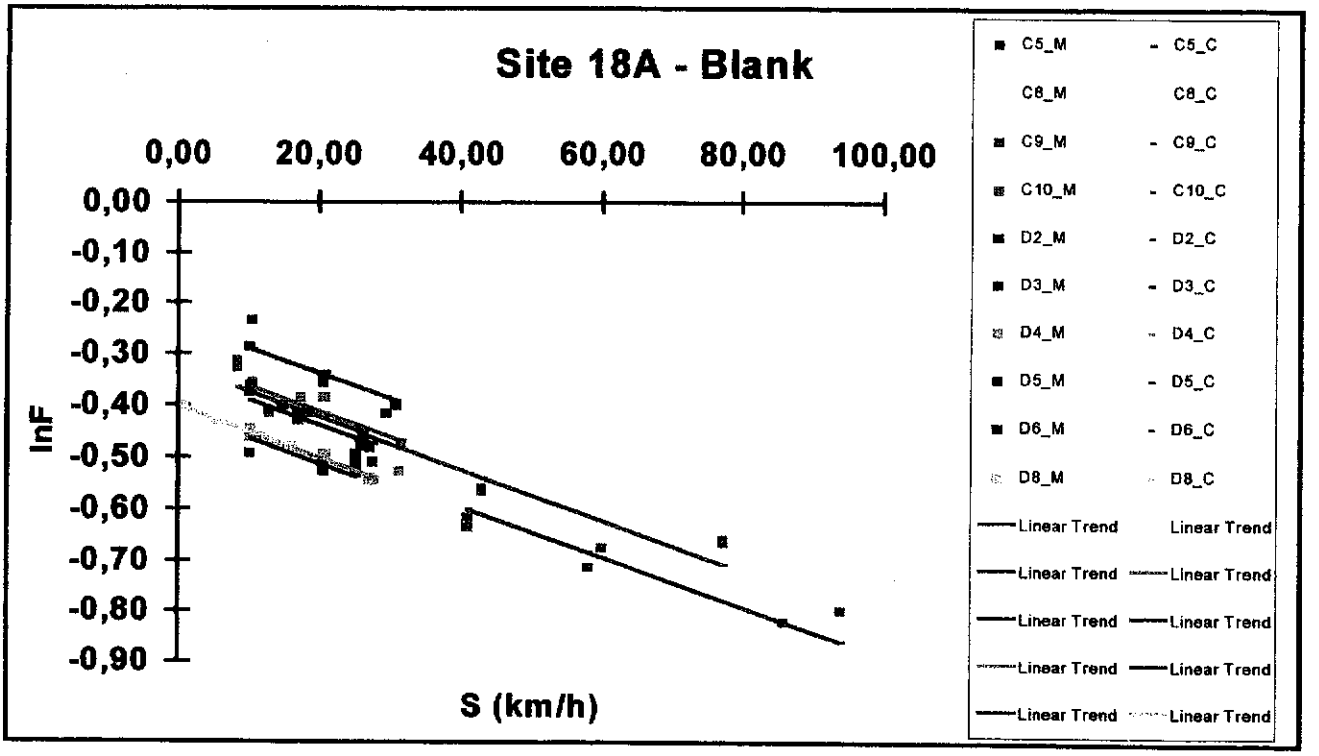

Figure 5 - Example of the fitting of exponential curves of equal slope to a series of data measured with different devices on a given half section

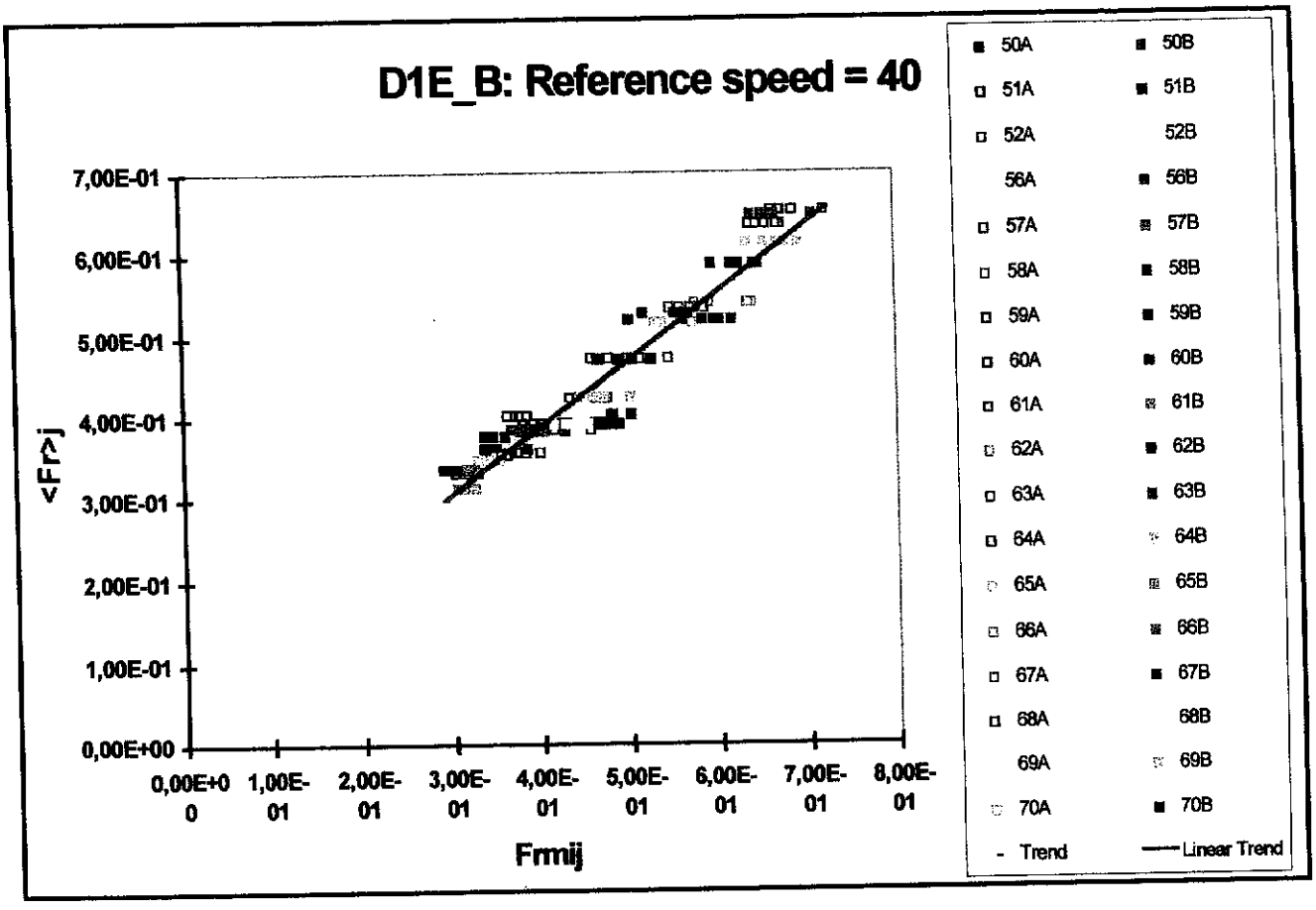

Figure 6 - Example of regression between individual friction measurements reduced to a common reference speed (S_R = 40 kmph) and the average value of these measurements for all devices ('Golden value') on a given half section

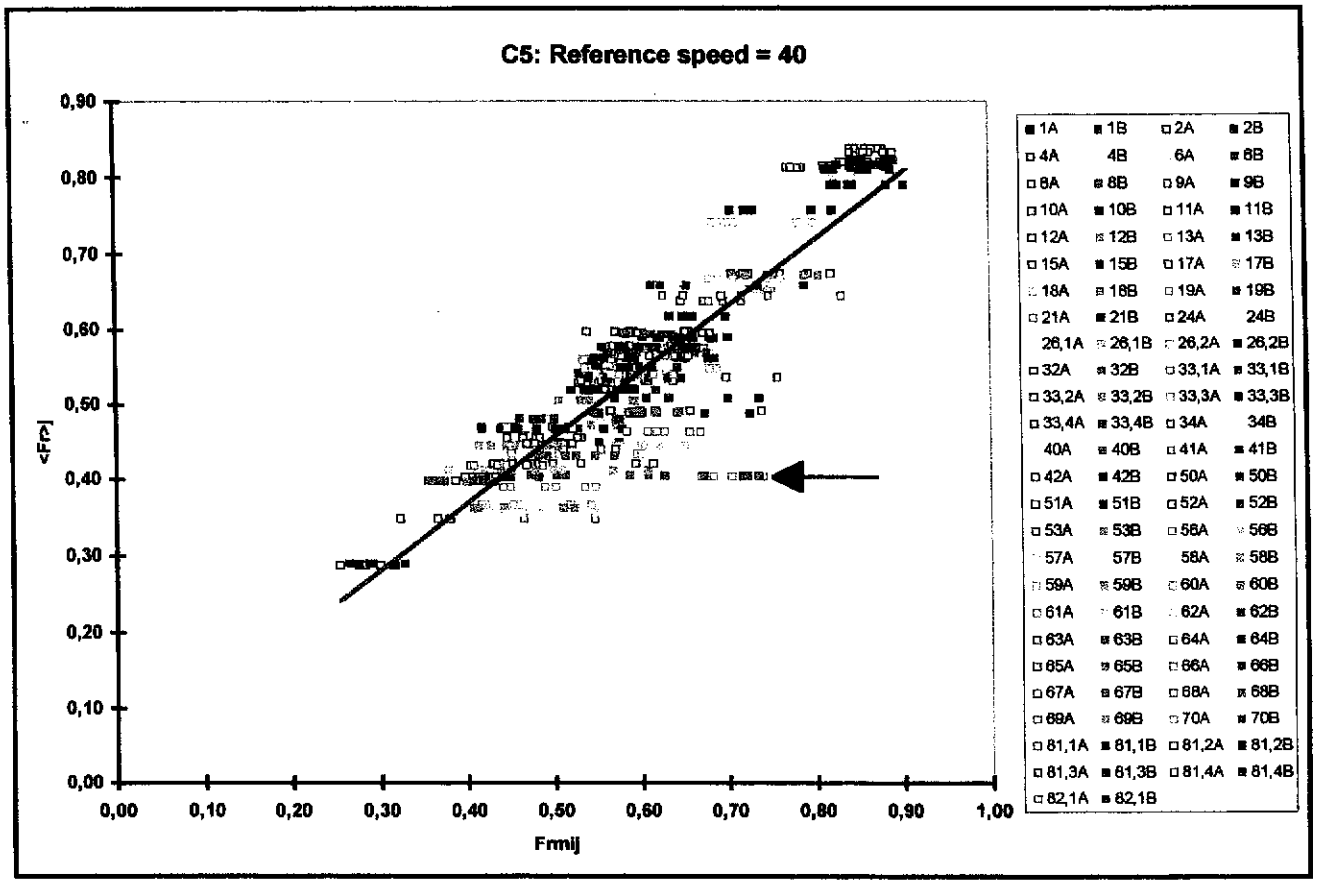

Figure 7 - Relation $\langle F_R \rangle_j$ vs F_{rmij} obtained on a site, with a series of outliers

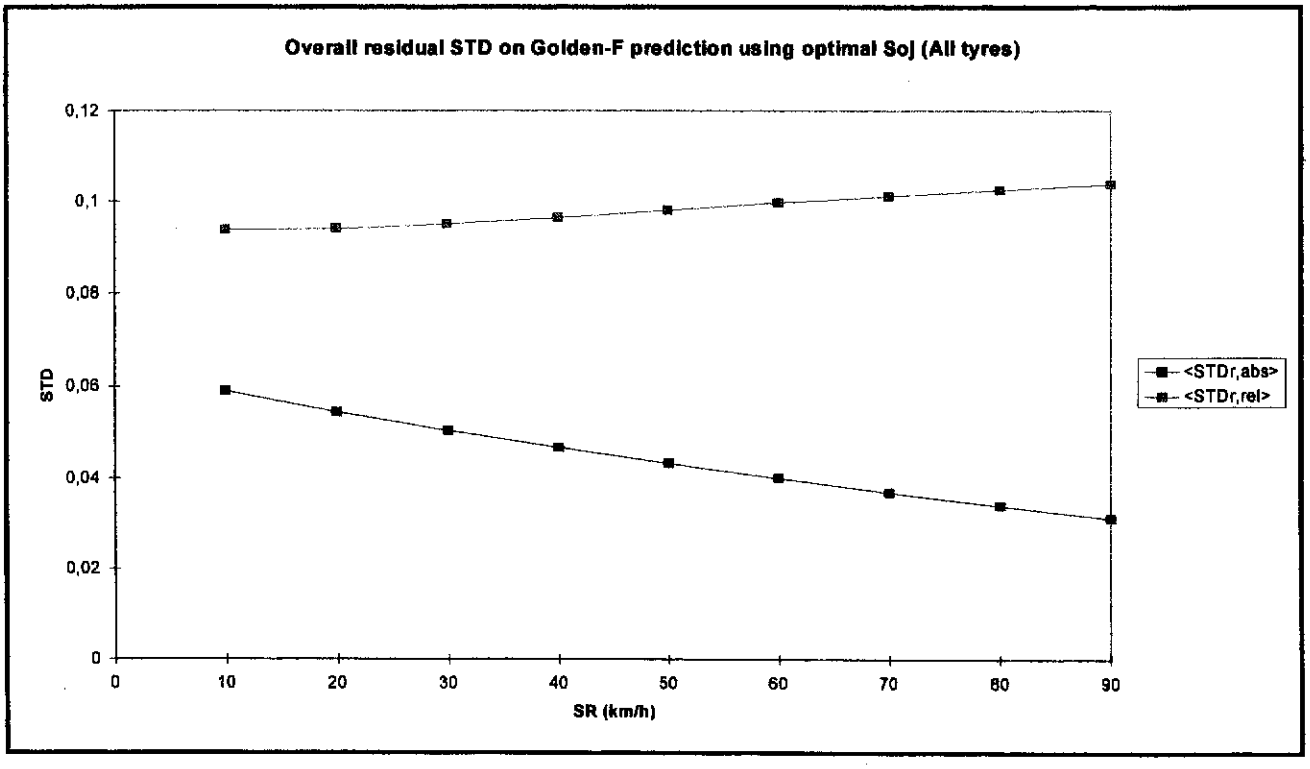

Figure 8 - Absolute and relative residual standard deviation of friction measurements from exponential curves of equal common slope per site

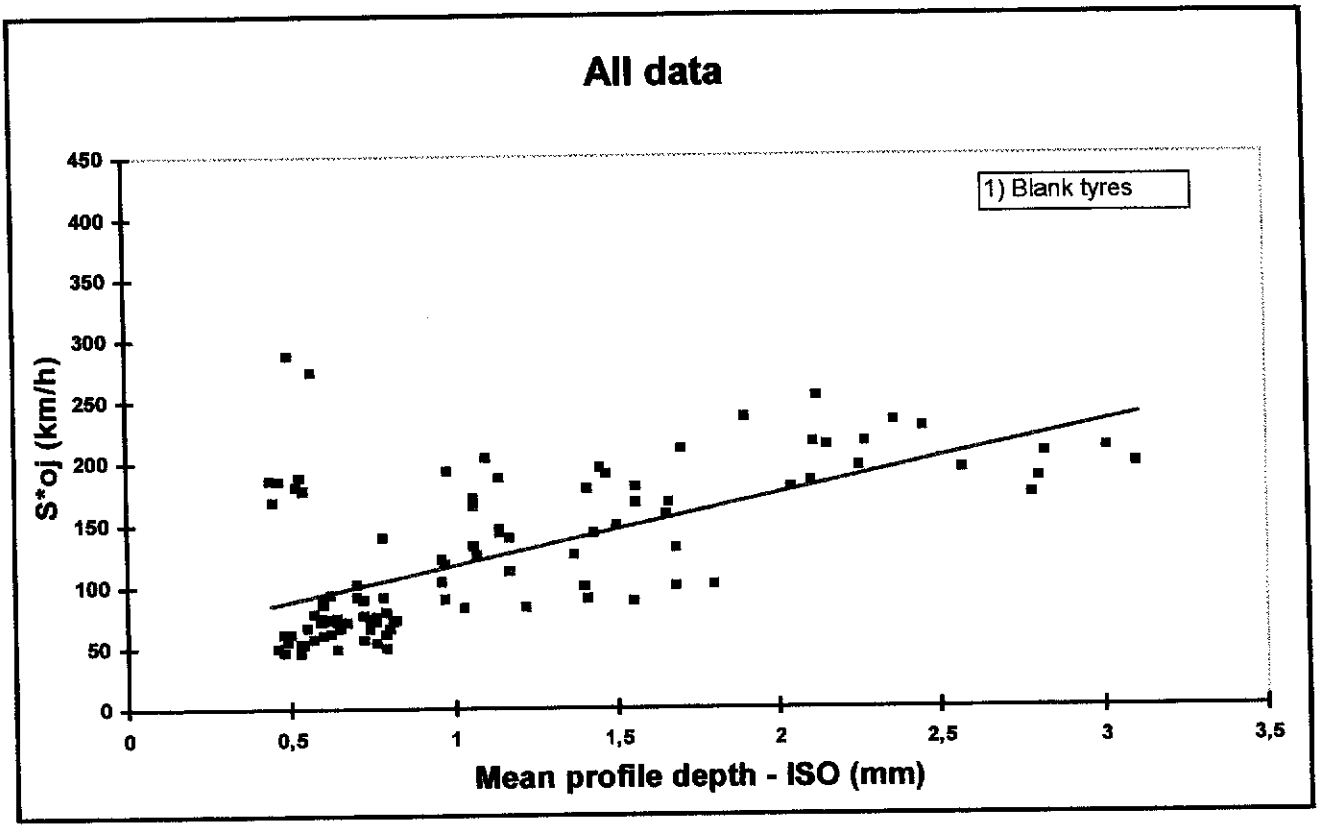

Figure 9 - Relation between fitted common values S_{oj}* and texture measurement Tiso for the devices with smooth tyres

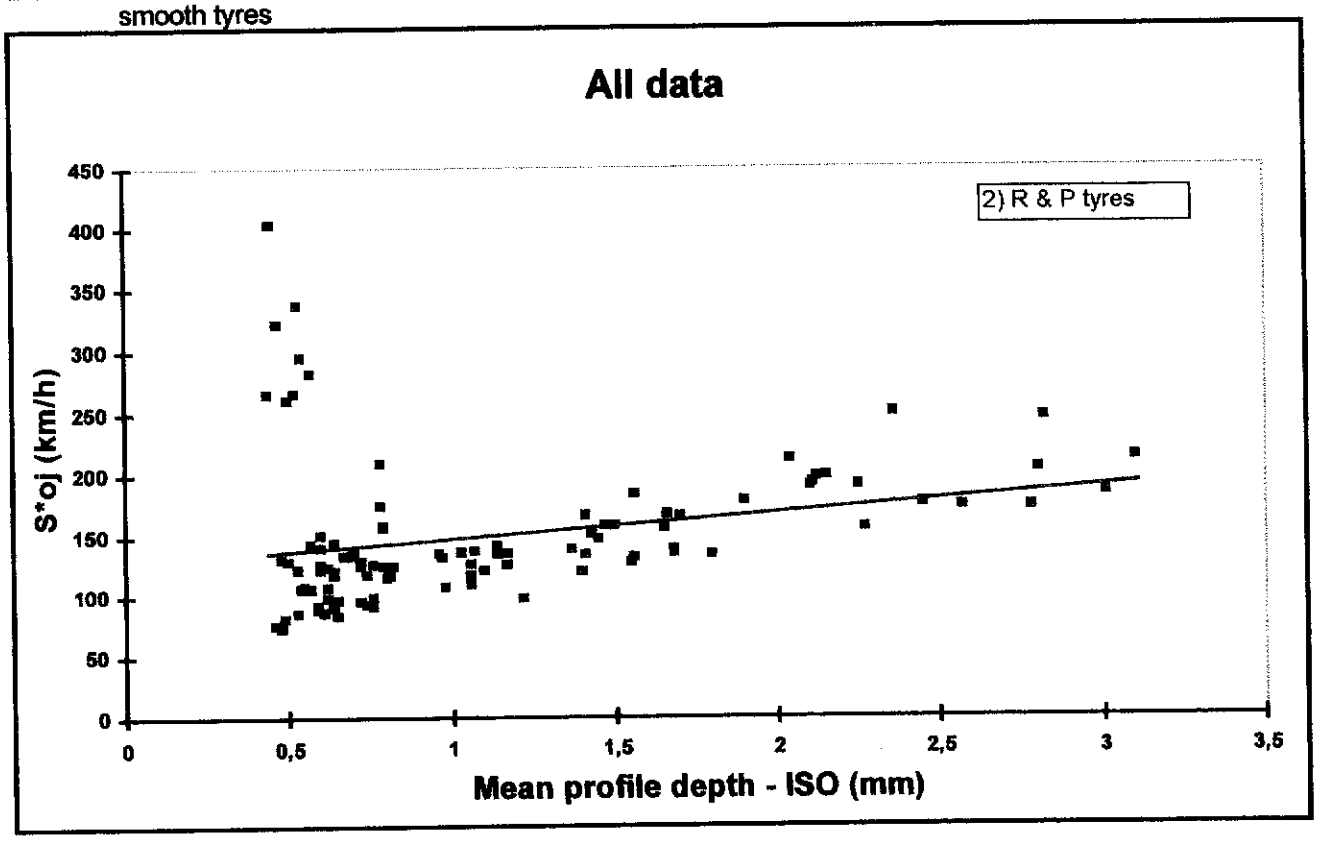

Figure 10 - Relation between fitted common values S_{oj}* and texture measurement Tiso for the devices with patterned tyres

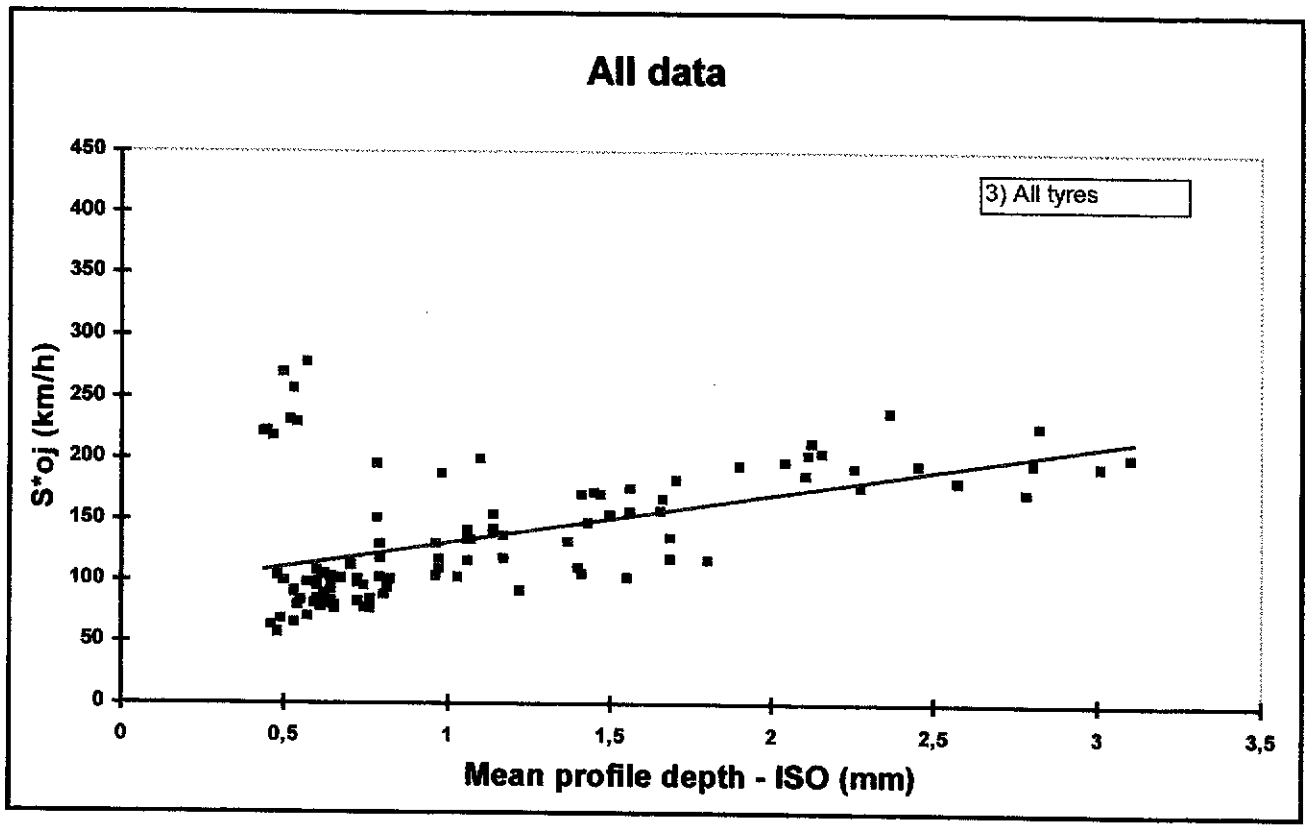

Figure 11 - Relation between fitted common values S_{oj}* and texture measurement Tiso for all devices, regardless of tyre type

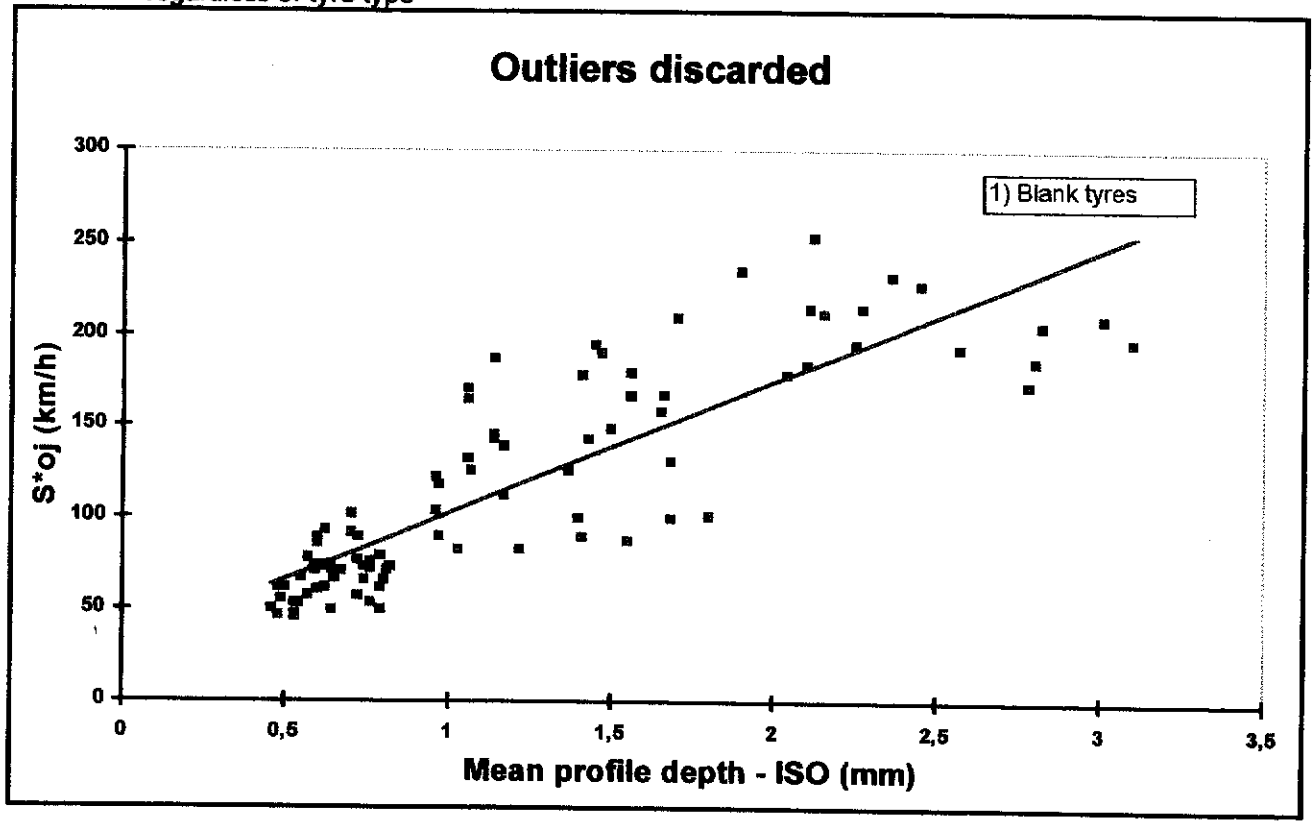

Figure 12 - Relation S_{oj}* vs T_{iso} trimmed of outliers (smooth tyres)

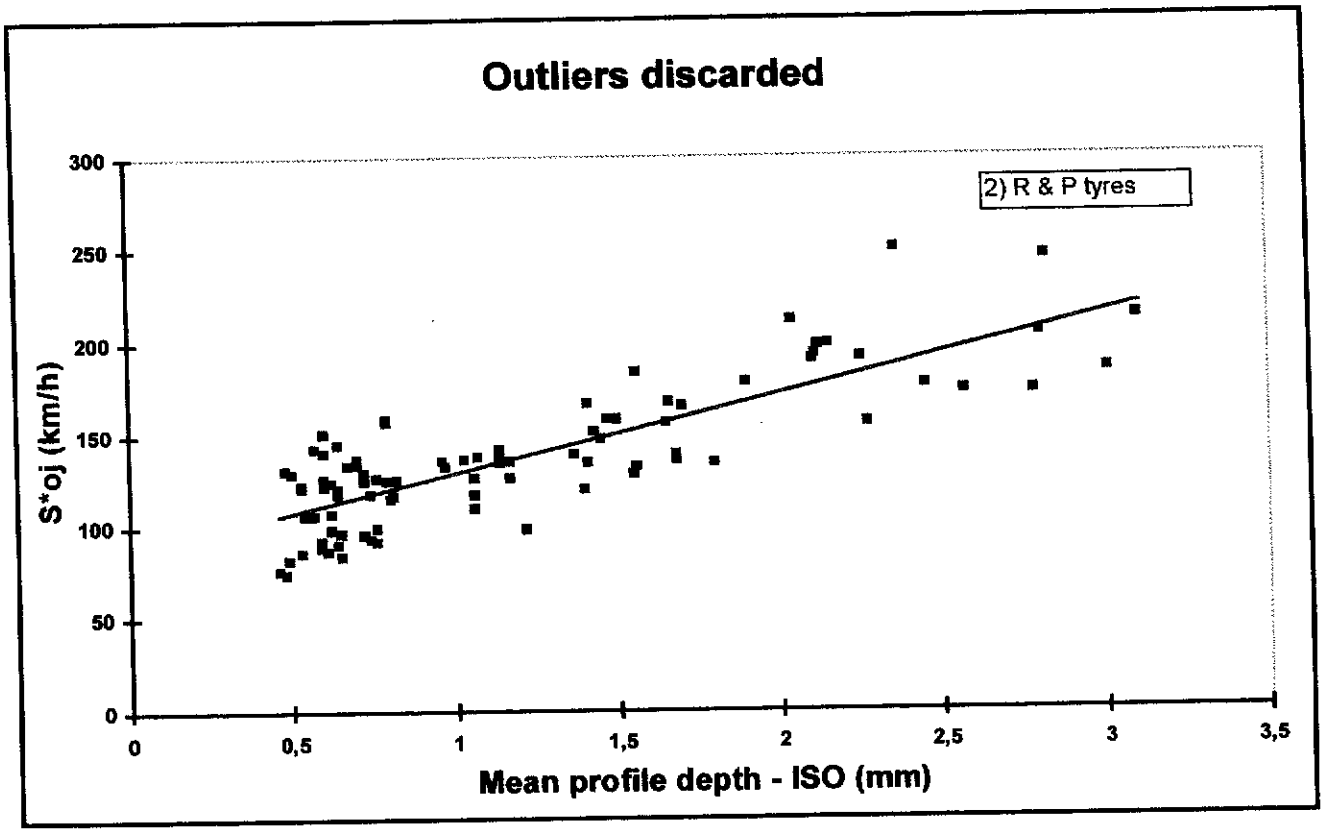

Figure 13 - Relation S_{oj}* vs T_{iso} trimmed of outliers (patterned tyres)

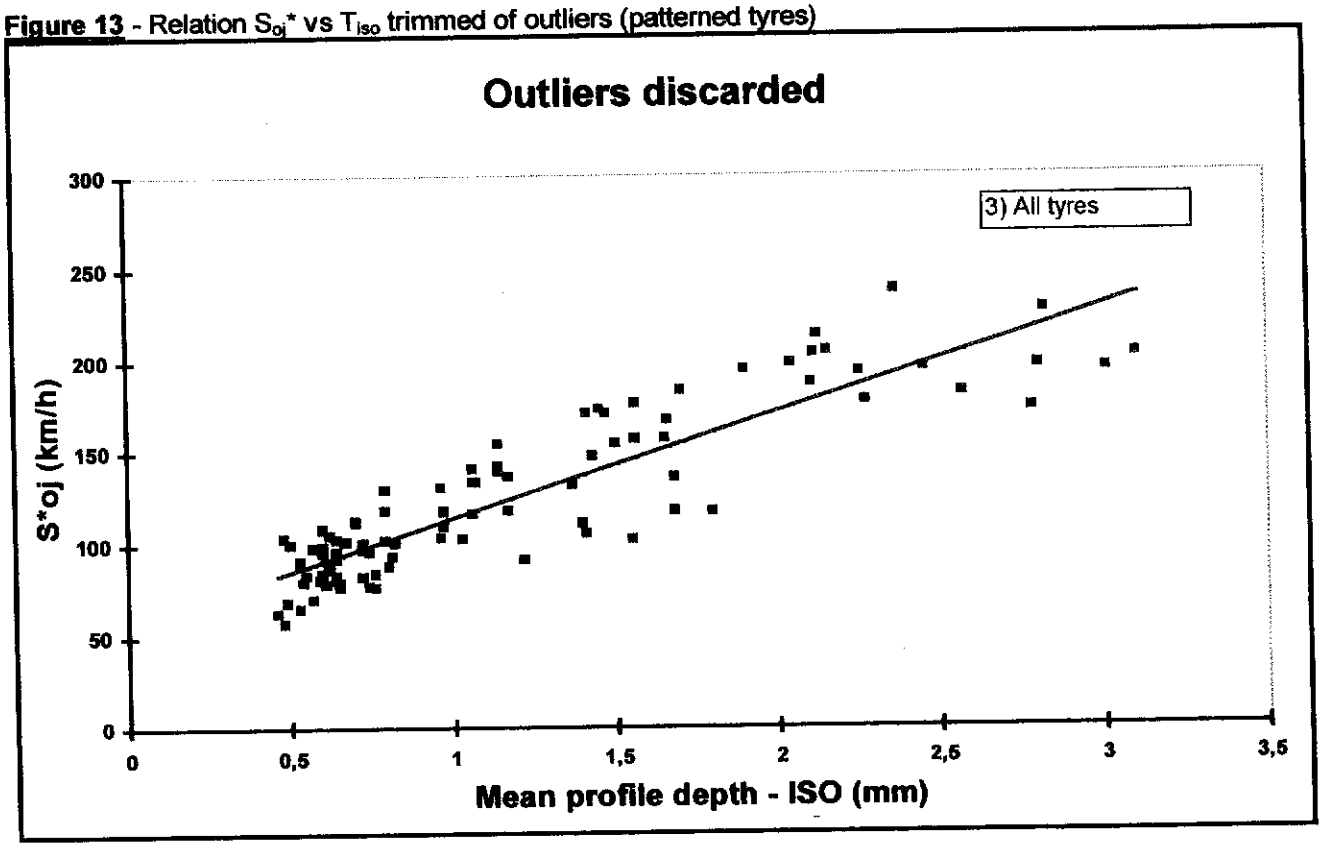

Figure 14 - Relation S_{oj}* vs T_{iso} trimmed of outliers (all tyres)

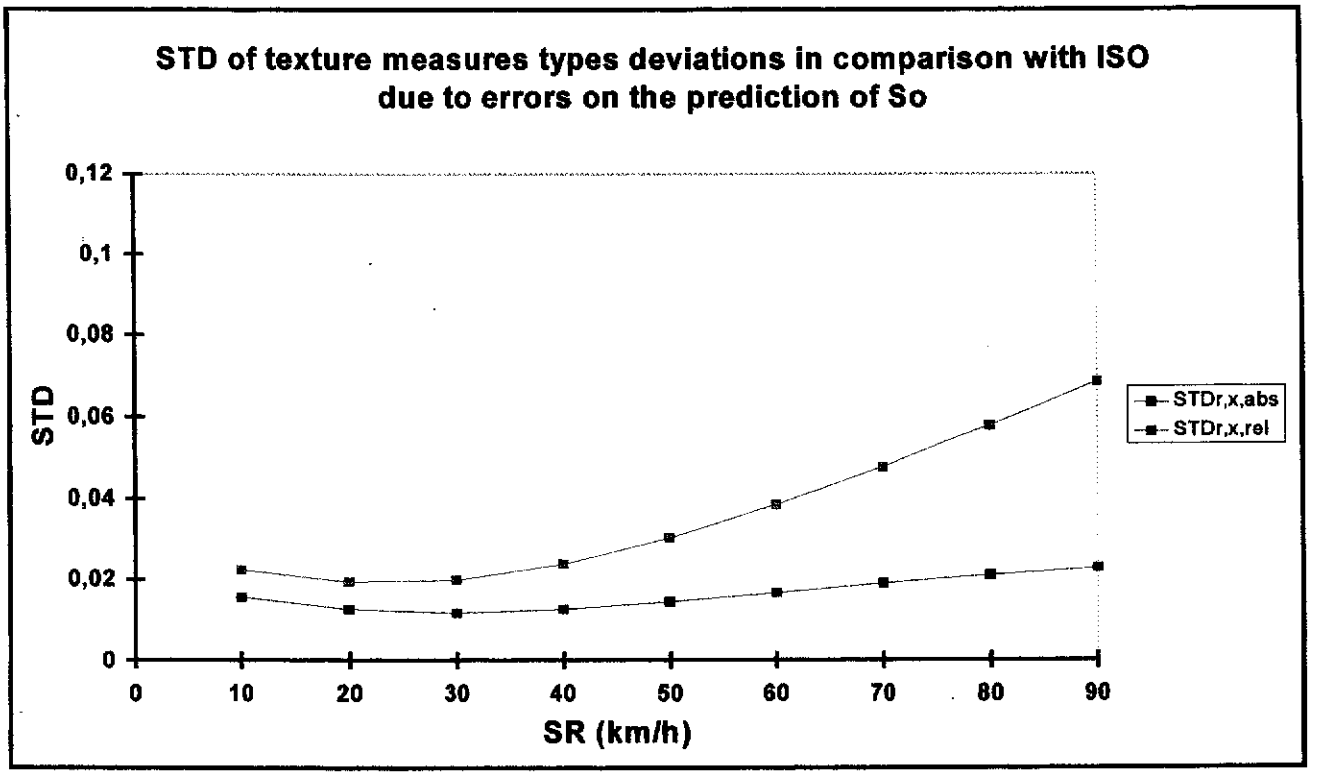

Figure 15 - Standard deviation of errors in EFI if S_{oj}* is predicted with a random error, as a function of the reference speed considered (single formula for all tyres to predict S_{oj}* from T_{iso})

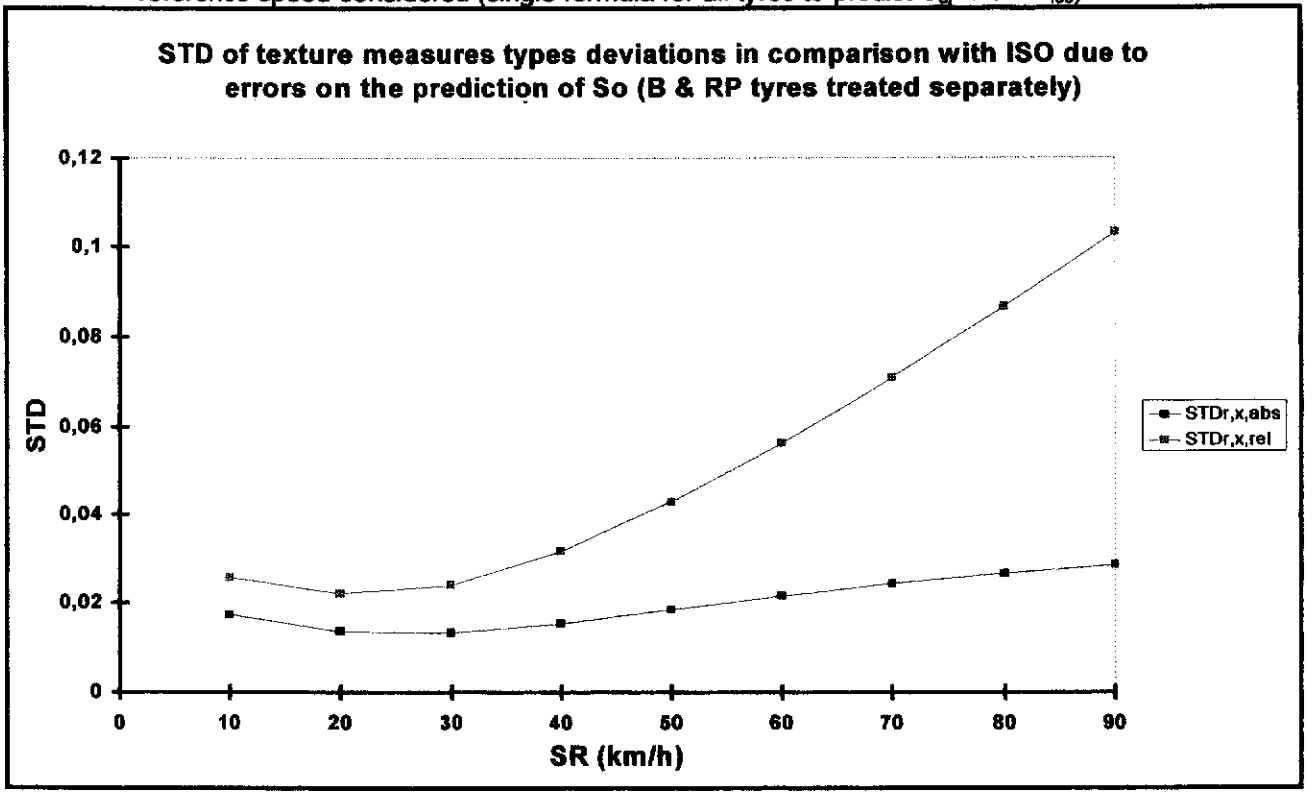

Figure 16 - Standard deviation of errors in EFI if S_{oj}* is predicted with a random error, as a function of the reference speed considered (different formulas for the two tyre types to predict S_{oj}* from T_{iso})

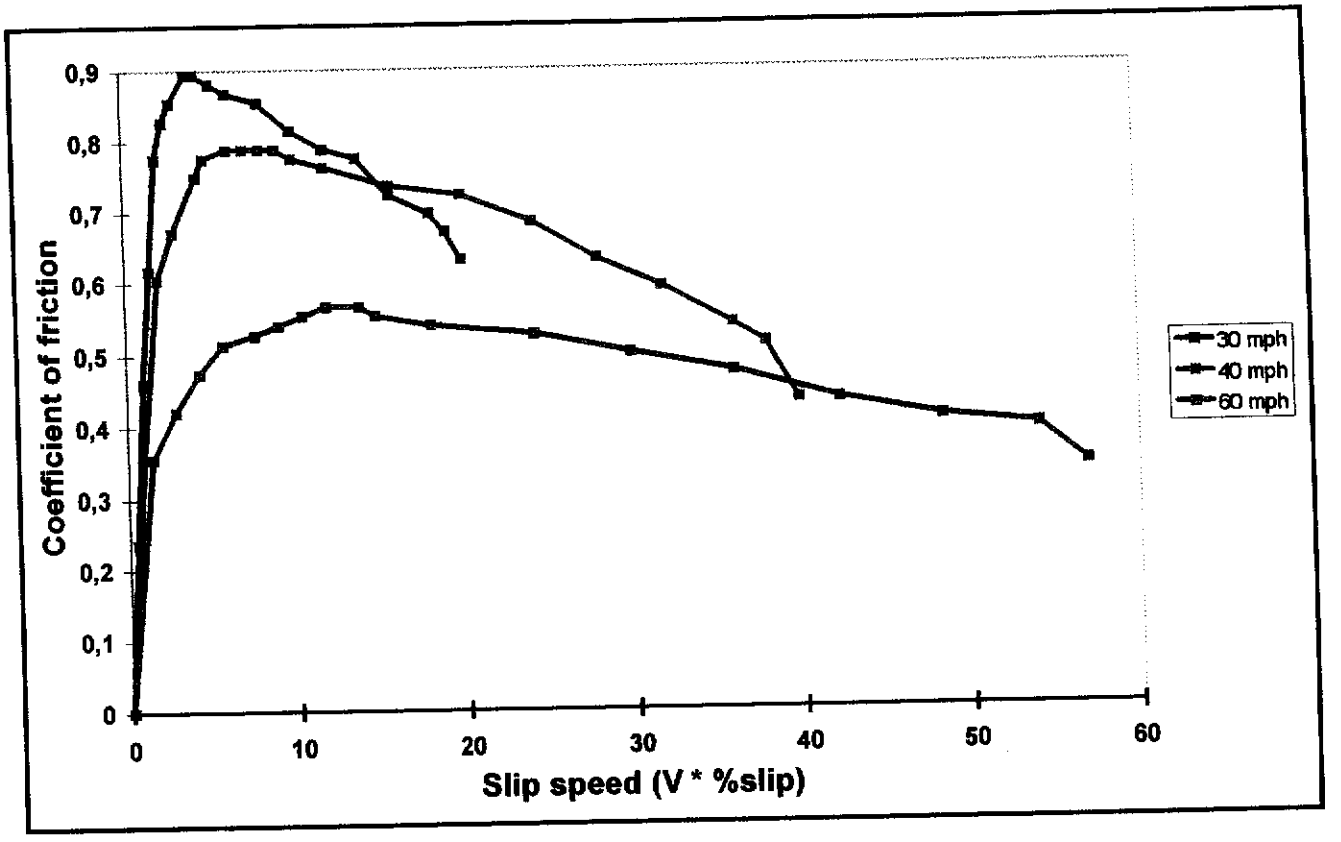

Figure 17 - Series of measurements showing that the friction coefficient depends on two independent variables: measuring speed and slip angle - after W.B. HORNE, quoted by Z. RADO **[ref. 3]**

PIARC model (Constant slip ratio)

$$F = F_O \; e^{-\frac{V}{V_O}}$$

RADO's model (Constant vehicle speed)

$$F = F_O' \; e^{-(k \log \frac{\tau}{\tau_m})^2}$$

General model

$$F = F_O'' \; e^{-\frac{V}{V_O} - (k \log \frac{\tau}{\tau_m})^2}$$

Figure 18 - Models of equations for the variation of the friction coefficient with speed (V), with the slip angle (τ), or with both

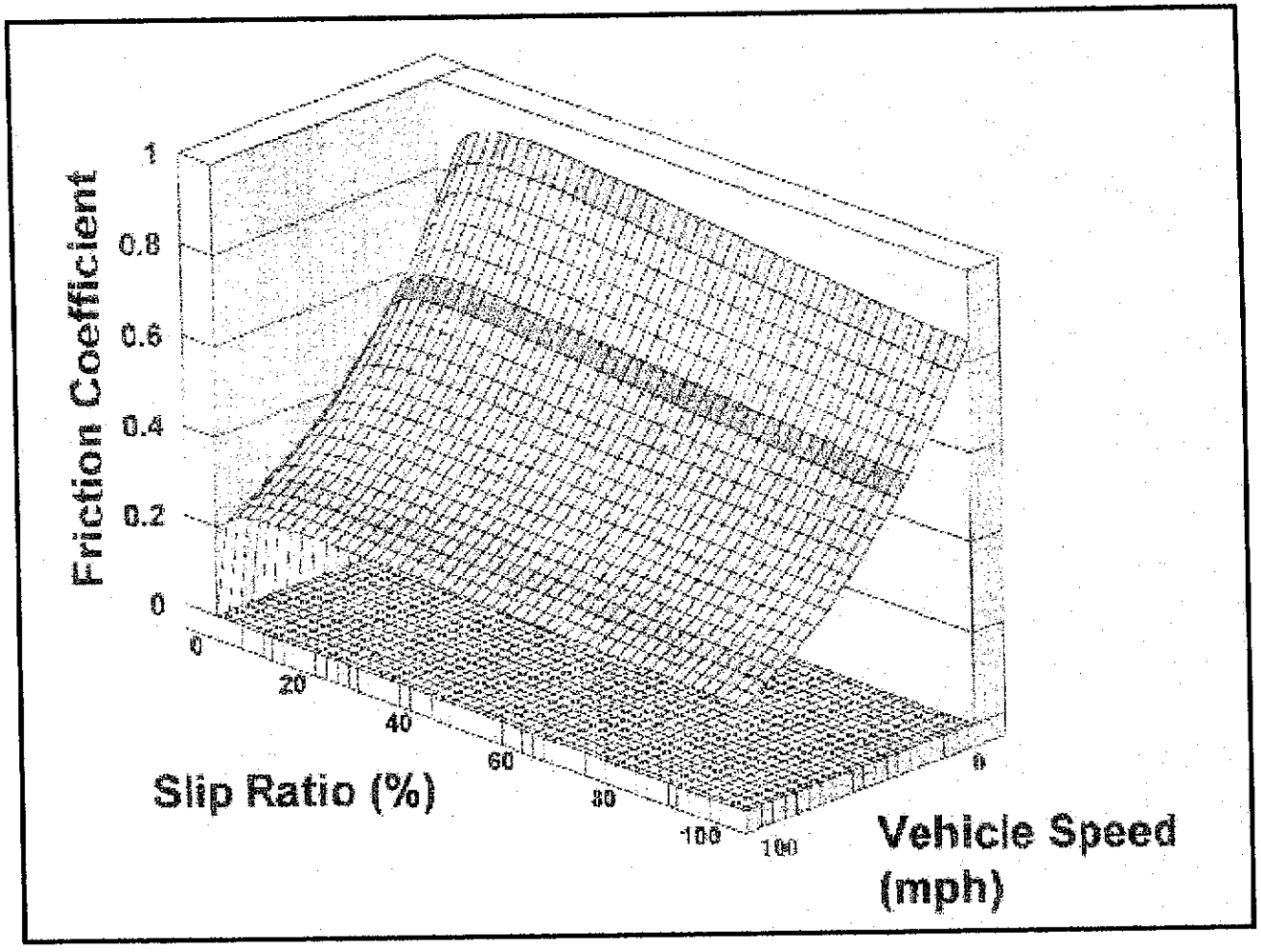

Figure 19 - Three-dimensional representation of the general model

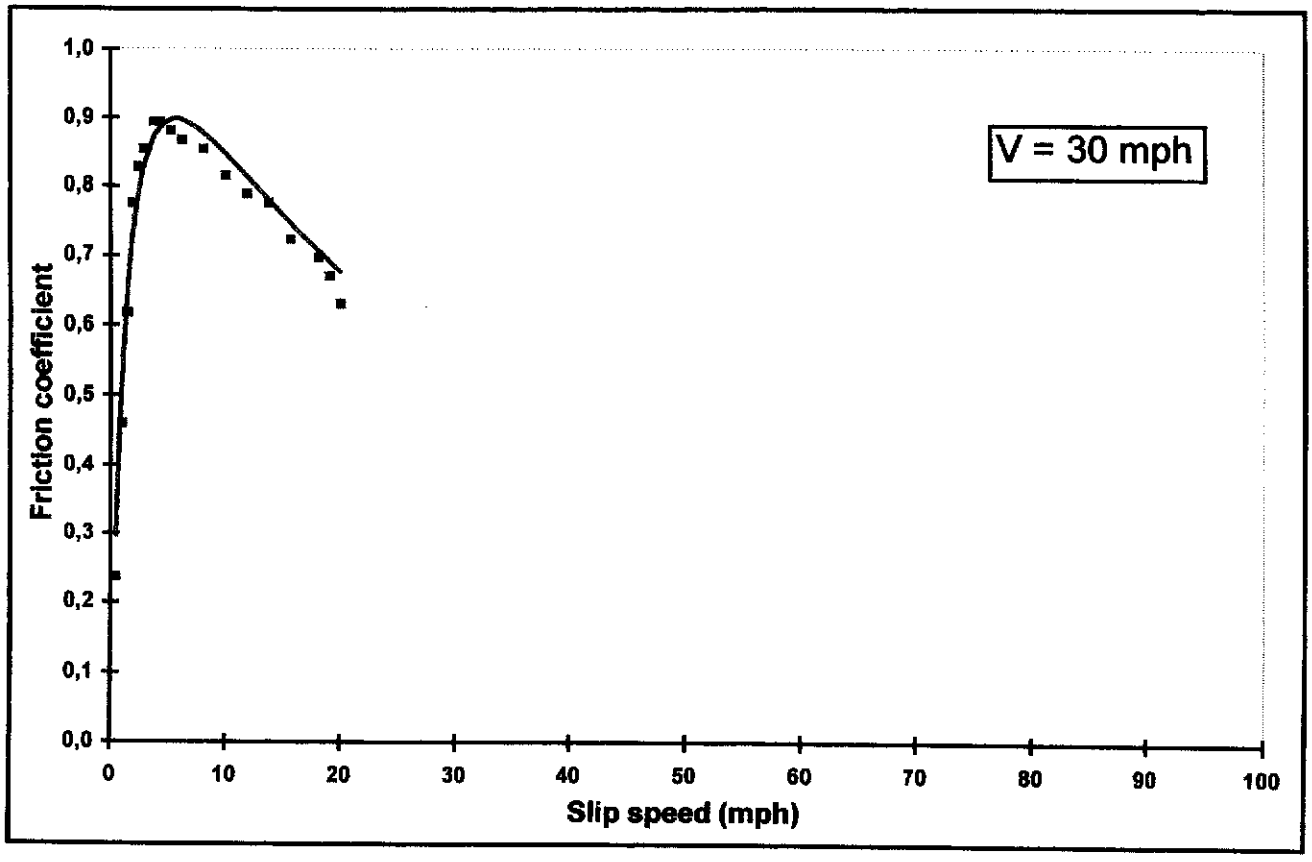

Figure 20 - Application of the general model to the data of figure 17

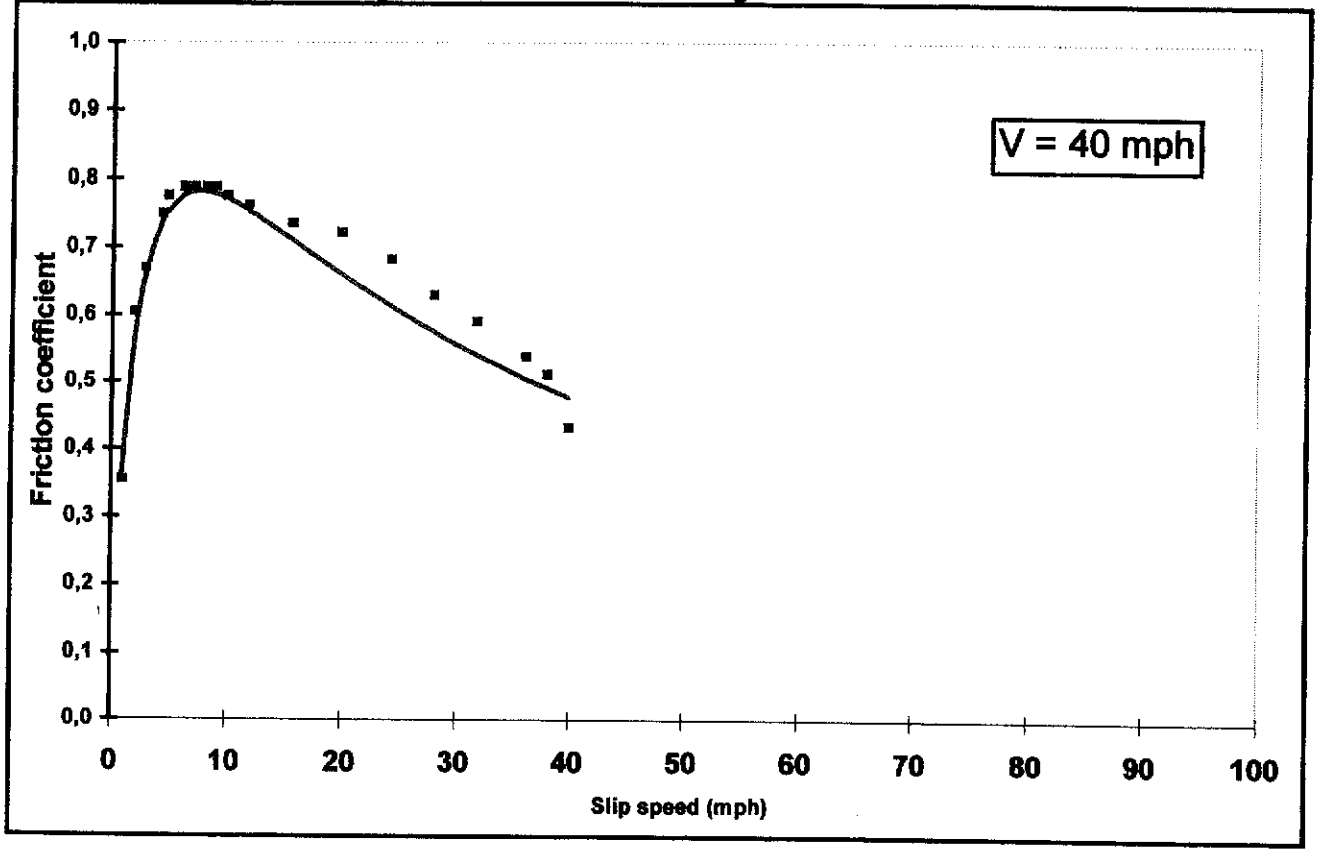

Figure 21 - Application of the general model to the data of figure 17

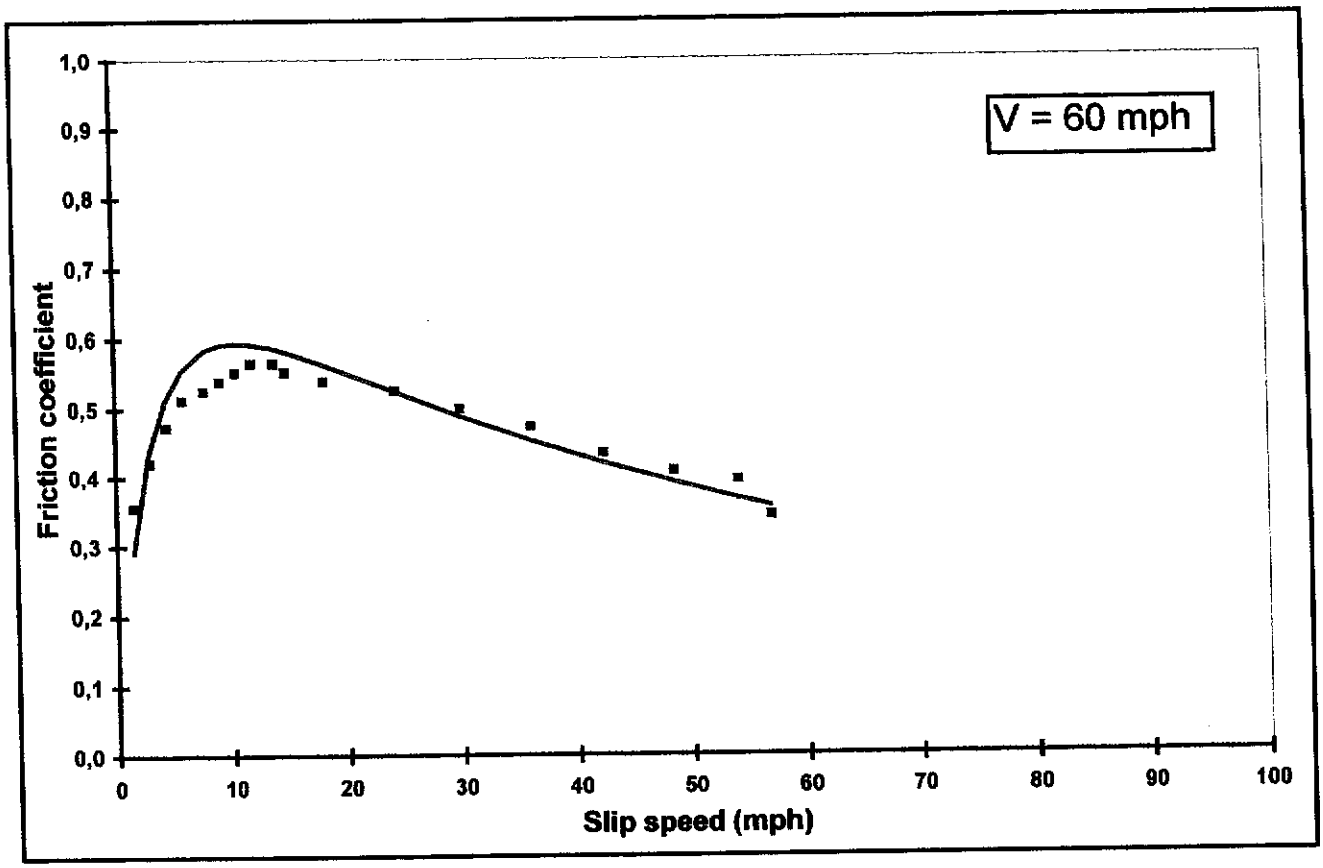

Figure 22 - Application of the general model to the data of figure 17

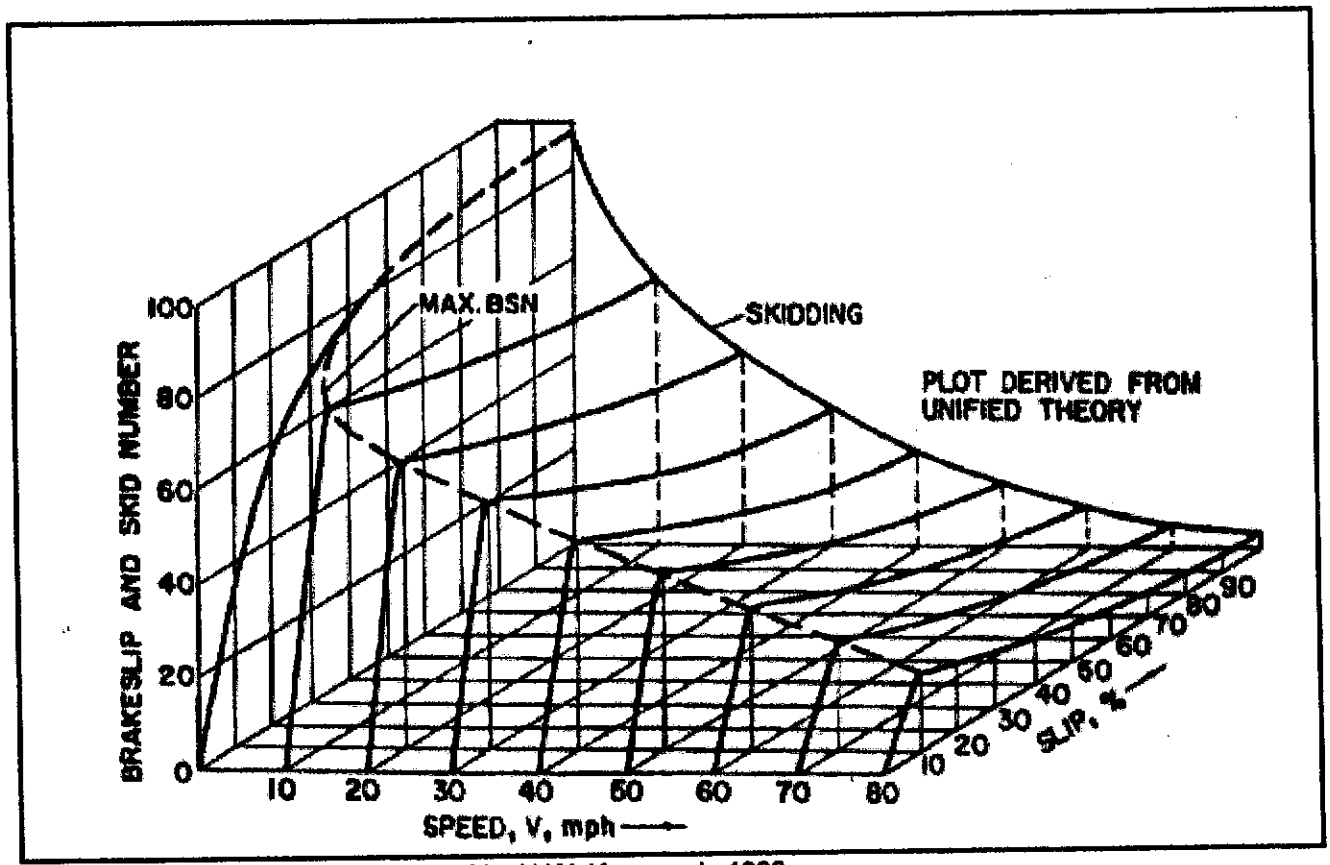

Figure 23 - Representation suggested by H.W. Kummer in 1966

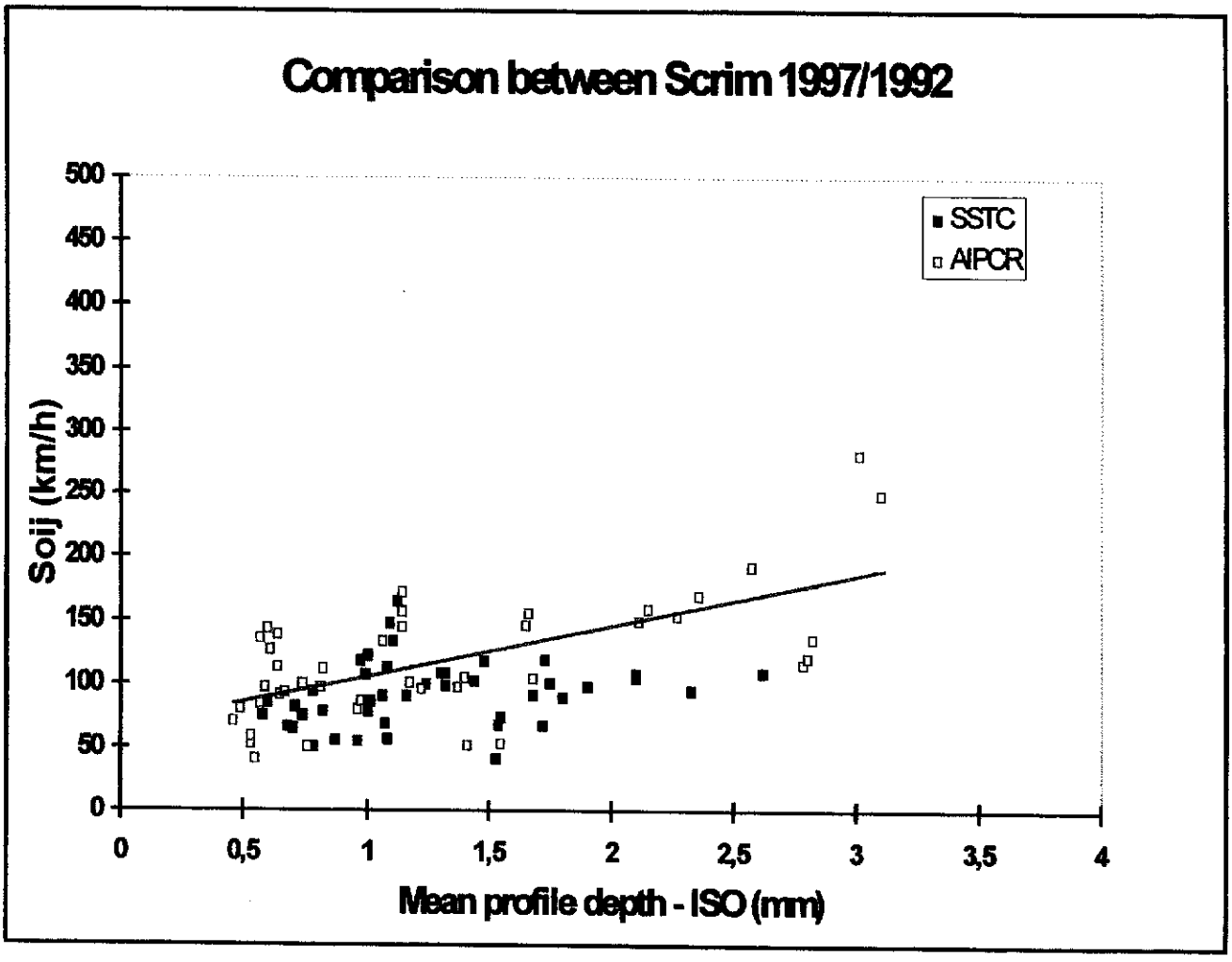

Figure 24 - Comparison of S_{oij} vs T_{iso} diagrams obtained on the PIARC and SSTC sites using the SCRIM measurements

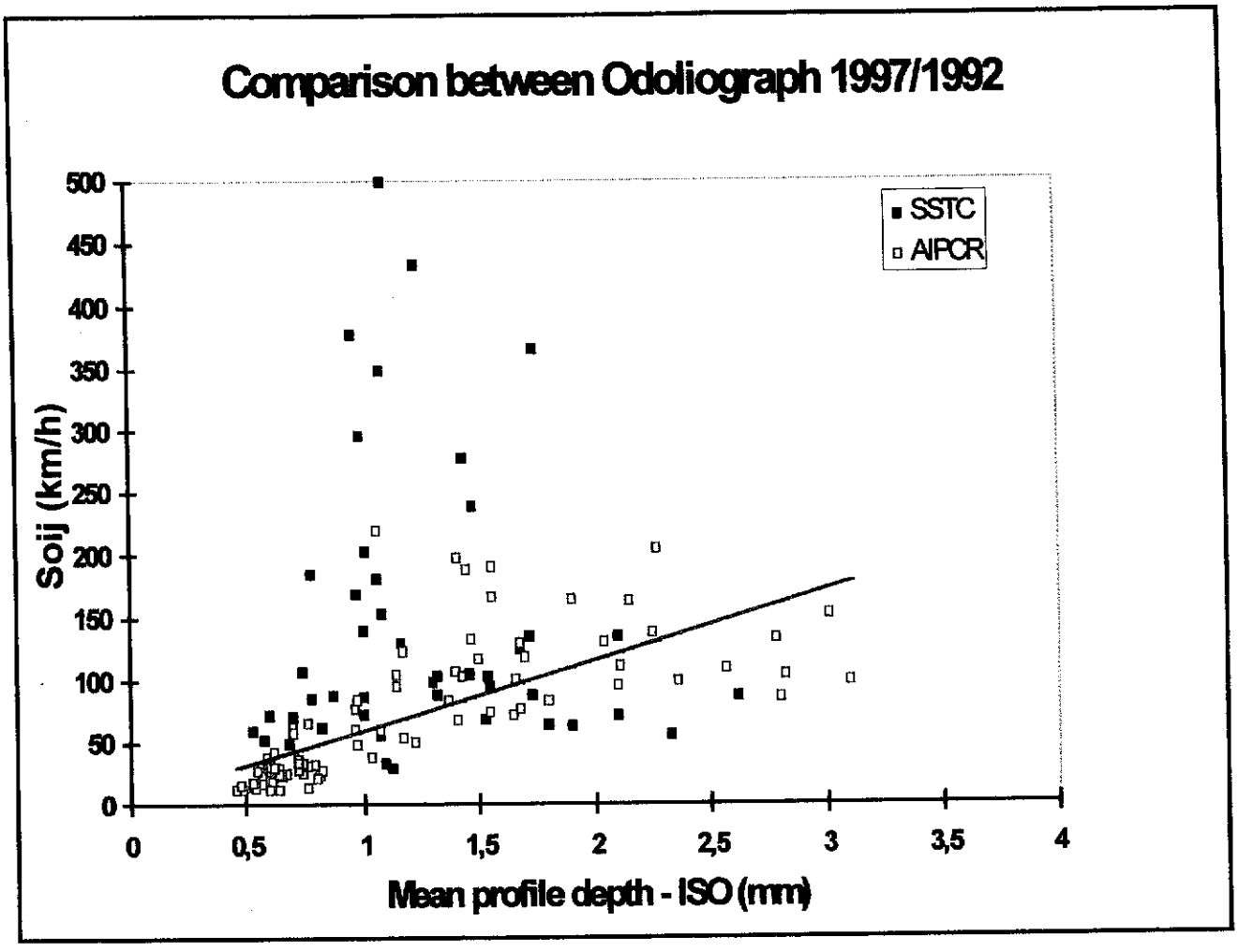

Figure 25 - Comparison of S_{oij} vs T_{iso} diagrams obtained on the PIARC and SSTC sites using the odoliograph measurements

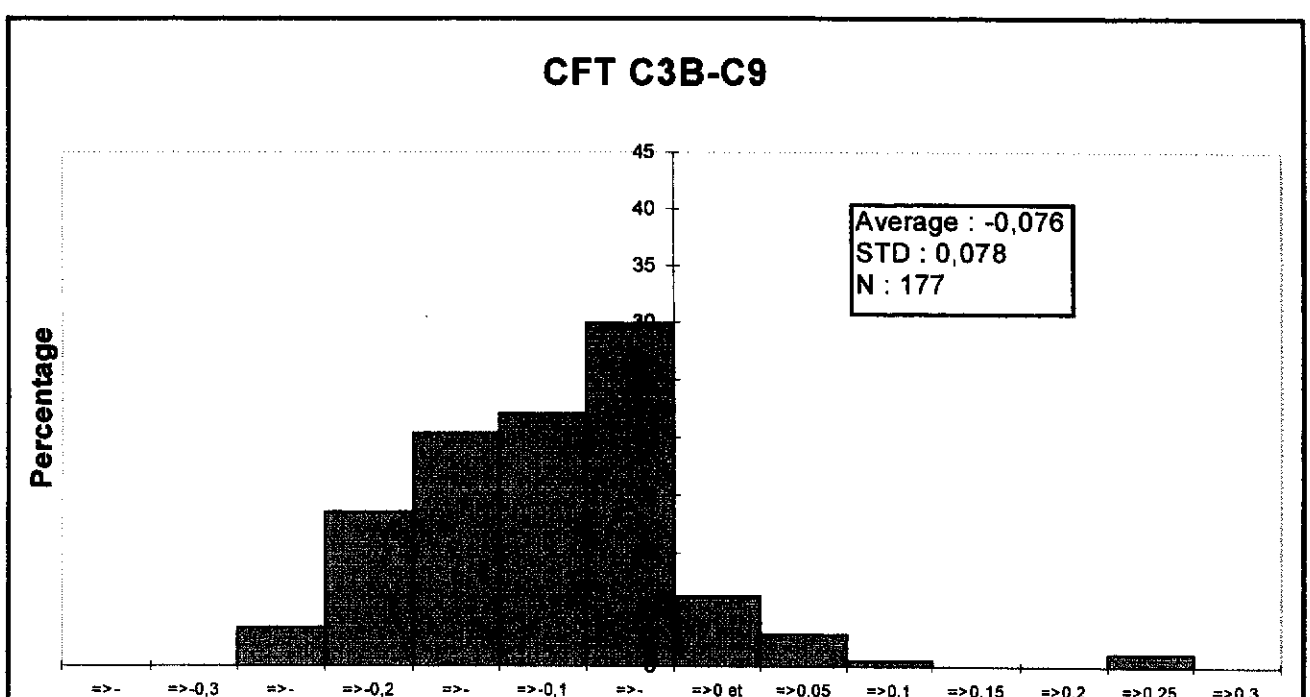

Figure 26 - Distribution of differences in SFC values provided by the SCRIM and the odoliograph measuring at the same speed on the same half site in the PIARC experiment

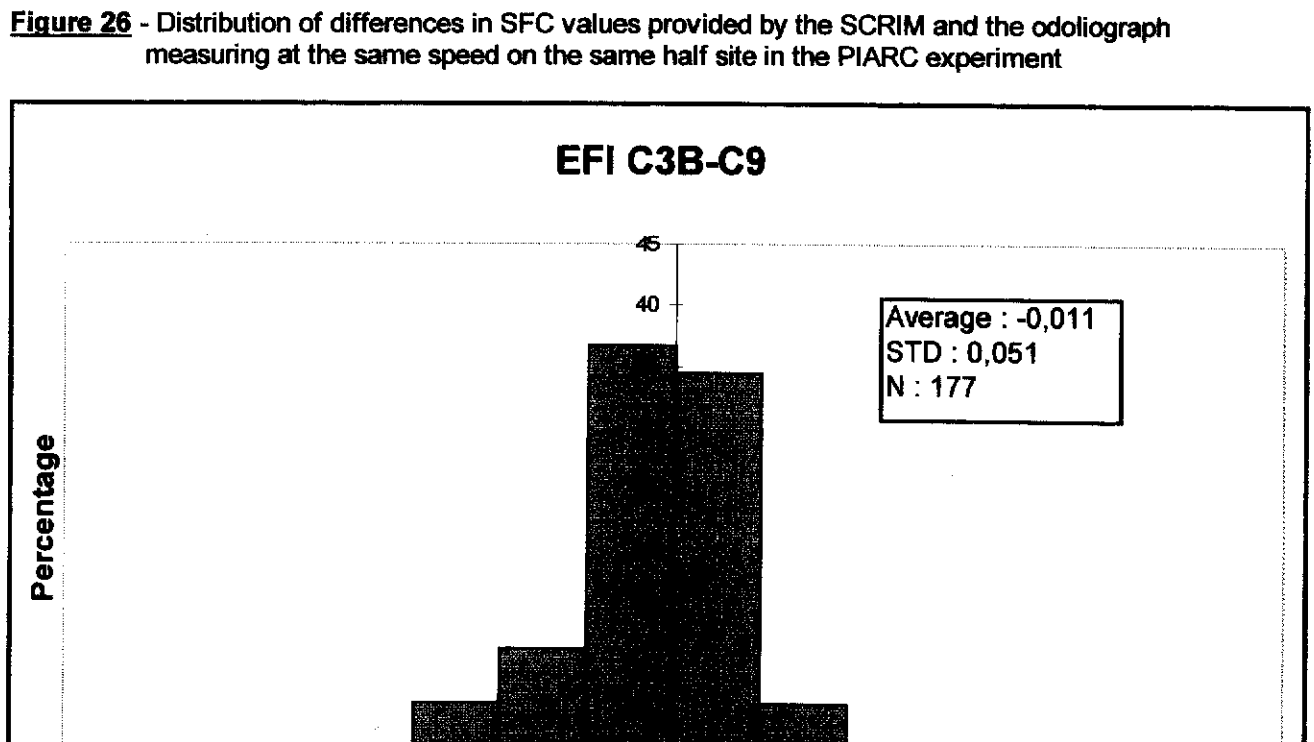

Figure 27 - Distribution of differences in EFI values found by the conversion of SCRIM and odoliograph measurements in the PIARC experiment

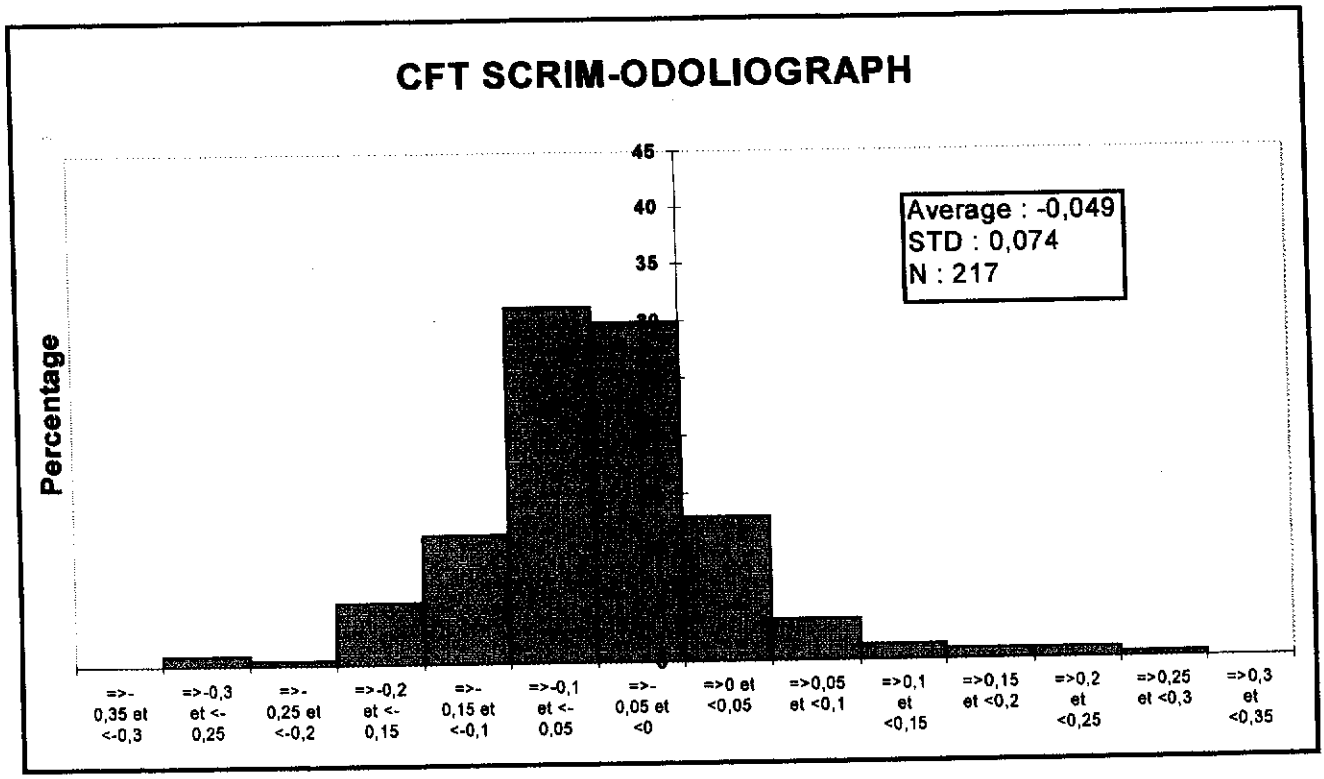

Figure 28 - Distribution of differences in SFC values provided by the SCRIM and the odoliograph travelling at the same speed on the same half site in the 1997 measurements

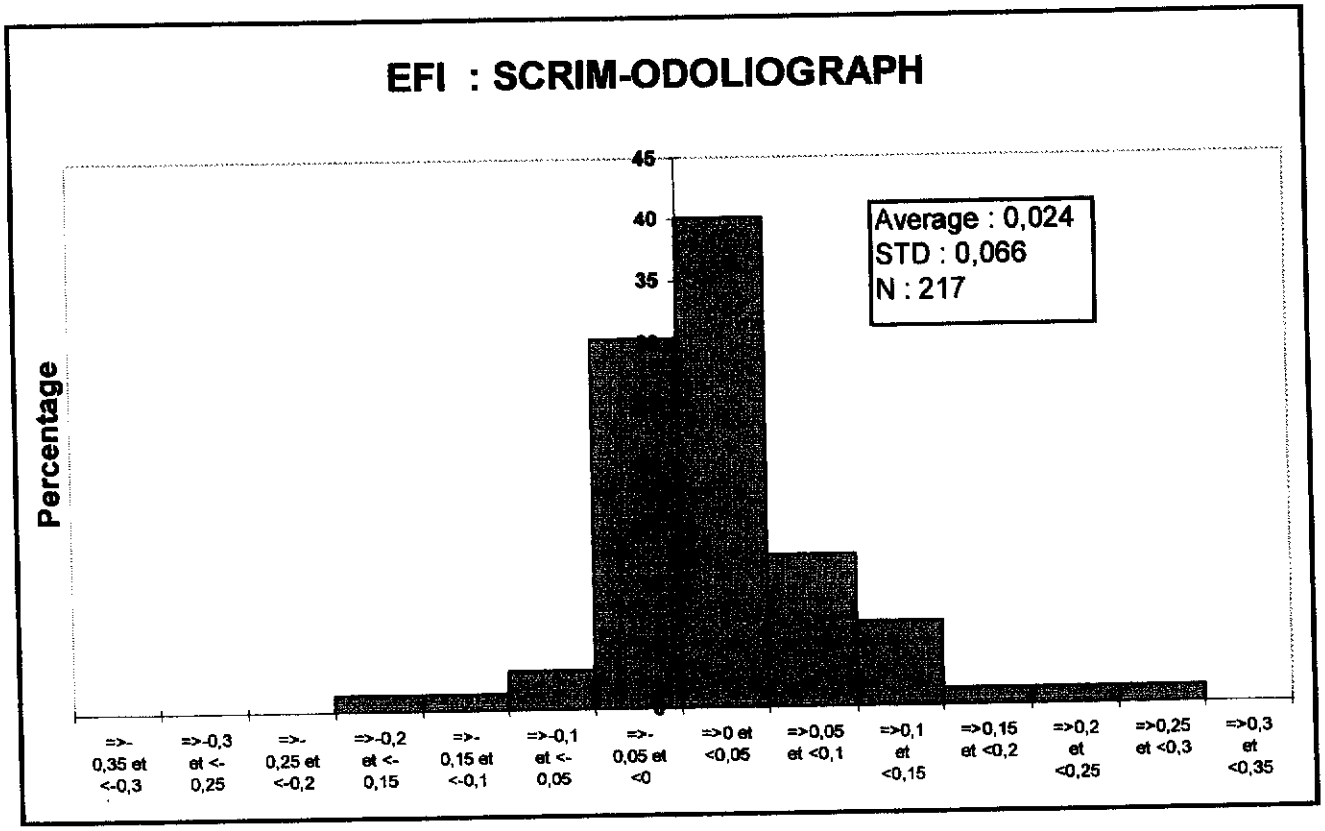

Figure 29 - Distribution of differences in EFI values found by the conversion of SCRIM and odoliograph results in the 1997 experiment

XIV. References

1. J.C.WAMBOLD et al., « International PIARC Experiment to Compare and Harmonize Texture and Skid Resistance Measurements », PIARC publication n°10.04.T, Paris, 1995.

2. « Characterization of Pavement Texture Utilizing Surface Profiles - Part 1: Determination of Mean Profile Depth, International Standard ISO 13473-1, 1996.

3. Zoltan RADO, « A Study of Road Surface Texture and its Relationship to Friction ». Ph.D. Thesis. The Pennsylvania State University,.1994.

4. H.W.KUMMER, "Unified Theory of Rubber and Tire Friction". Pennsylvania State University, Engineering Research Bulletin B-94, 1966.

5. "Precision of test methods - Determination of repeatability and reproducibility by inter-laboratory tests". International Standard ISO 5725, 1985.

XV. Appendixes

- **Appendix 1** is a CD-Rom containing the detailed results in the form of over 4,000 graphs and tables of figures, as well as the present report and a navigation programme allowing easy retrieval of specific data and cross-referencing between that data and the corresponding parts of the report.

- **Appendix 2** is the third draft, dated June 1998 and prepared after the May 25-26 discussions of CEN Group TC227/WG5 in Linköping, of the proposal for a standard on "Surface Characteristics - Determination of the European Friction Index (EFI)" (Reference : *CEN/TC227/WG5 N88E - Rev.3*).